

Distributed estimation of many-body Hamiltonians via punctured surface code

Linmu Qiao,^{1,*} Zhichun Ouyang,² and Sisi Zhou^{3,4,†}

¹*Department of Mechanical and Automation Engineering,
The Chinese University of Hong Kong, Shatin, Hong Kong*

²*Department of Physics, Hong Kong University of Science and Technology, Clear Water Bay, Hong Kong, China*

³*Perimeter Institute for Theoretical Physics, Waterloo, Ontario N2L 2Y5, Canada*

⁴*Department of Physics and Astronomy and Institute for Quantum Computing,
University of Waterloo, Ontario N2L 3G1, Canada*

We study how a punctured surface code can turn many local Z-type couplings into one protected logical signal for distributed quantum metrology, where the goal is to estimate a weighted average of the coupling strengths. We consider an ordinary planar patch with two X-cut holes and provide a distributed sensing protocol where all Z-type couplings correspond to the same nontrivial logical \bar{Z} for the punctured surface code. When the couplings are disjoint, we show that the relevant global condition is equivalent to the existence of a closed dual loop, called a *witness*, that has an odd number of intersections with every chain. Together with a local clean opening condition, this witness criterion gives a concrete punctured-code construction in which all signal chains implement the same nontrivial logical \bar{Z} . For three-body interactions with overlapping supports, we also identify the class of interactions where our punctured surface code protocol applies. Overall, our results provide a novel, noise-robust distributed sensing protocol for many-body interactions, with corresponding topological design criteria.

I. INTRODUCTION

Quantum sensing can gain from entanglement, especially when the goal is not to estimate every local parameter separately, but one chosen linear functional of them. In distributed quantum sensing [1–10], a basic task is to estimate

$$q = \sum_{\alpha} s_{\alpha} \lambda_{\alpha}, \quad (1)$$

where the weights s_{α} are known and the couplings λ_{α} are unknown. This task includes weighted averages and other spatial modes of a field. In ideal models, entangled probes can reach the Heisenberg limit for such a target quantity [2–5]. However, the best known protocols usually rely on long-range coherence across the whole sensor network, and this makes them sensitive to noise and imperfect control. This leads to a natural question: can the same sensing task be realized in a form that is protected by quantum error correction [11–22]?

In this work, we study this question for a family of local many-body Z-type couplings. The sensing Hamiltonian has the form

$$H = \frac{1}{2} \sum_{\alpha} \lambda_{\alpha} \prod_{j \in S_{\alpha}} Z_j, \quad (2)$$

where λ_{α} is an unknown coupling strength, S_{α} is a known local connected support, and Z_j is the single-qubit Pauli Z on qubit j . Thus each term is a product of Z operators over a known support. Our target is still the weighted

sum in Eq. (1). We do not try to estimate all couplings separately. Instead, we ask whether these different physical signal terms can be made to act as one protected logical generator, so that the target quantity q is written onto a single logical qubit.

Our setting is a planar surface code [23–28]. Data qubits live on edges of a lattice. X-type stabilizers live on vertices, and Z-type stabilizers live on faces. Let E be the set of data-qubit edges. In the main text, each signal support S_{α} is represented by a connected simple primal path $c_{\alpha} \subseteq E$. That is, c_{α} runs along adjacent primal edges, has no self-intersection, and forms one connected piece. In the algebraic topology language used later in the Supplemental Material, c_{α} is the corresponding 1-chain in $C_1(G; \mathbb{F}_2)$. We then write

$$Z(c_{\alpha}) := \prod_{e \in c_{\alpha}} Z_e, \quad (3)$$

where Z_e is the single-qubit Pauli Z on the qubit on edge e . In this way, c_{α} labels the support, while $Z(c_{\alpha})$ is the corresponding multi-qubit Z string. The Hamiltonian in Eq. (2) can therefore be written as

$$H = \frac{1}{2} \sum_{\alpha} \lambda_{\alpha} Z(c_{\alpha}). \quad (4)$$

Our distributed estimation strategy is to find a punctured surface code such that $Z(c_{\alpha})$ are logical operators and can be detected jointly.

We now modify the planar patch by puncturing two rough holes, denoted by R_0 and R_1 . In the usual surface-code language, these are two X-cut holes or defects. Equivalently, they are created by turning off star checks in two connected regions. Below, we also use witness-guided regions Ω_0 and Ω_1 , which contain R_0 and R_1 , respectively, and help identify the rough holes. After these

* linmuqiao3@gmail.com

† sisi.zhou26@gmail.com

two rough holes are introduced, a primal Z path is allowed to start on R_0 and end on R_1 . Here and below, this means that the endpoint lies on the rough boundary of R_i , the part of R_i adjacent to the active code region. The corresponding operator $Z(c)$ is then a candidate logical \bar{Z} on the code space.

To represent the same logical operator \bar{Z} , the signal supports $\{c_\alpha\}$ need not look the same in real space. They may have different shapes, different lengths, and different locations on the patch. What matters is not their local form, but their action on the code space. This leads to the central question of the paper: when do all operators $\{Z(c_\alpha)\}$ act as the same nontrivial logical \bar{Z} on the code space?

Once all relevant signal chains act as the same logical \bar{Z} , the sensing task becomes a logical Ramsey experiment. We prepare a logical superposition state. The unknown couplings then build up one logical phase, which is exactly the weighted sum q . This phase can be accumulated in two closely related ways. In a parallel picture, several compatible signal terms contribute to the logical phase during the same sensing window, with their weights set by the local control. In a sequential picture, one lets different signal supports contribute one after another, with their weights set by the chosen time schedule. These two pictures lead to the same target quantity, but they highlight different ways to implement the protocol. Because the phase is stored at the logical level, the scheme also inherits the usual protection of the surface code against errors that remain correctable during the sensing process. The paper then develops this idea in stages. We start from a simple motivating planar example and the logical picture behind it. We next explain the sensing protocol. We then turn to the topological criterion and the constructive synthesis of suitable rough regions. We close with the main limitations of the method, its caveats, and the issue of overlapping supports.

II. A MOTIVATING EXAMPLE

Figure 1 fixes the geometric language used in the rest of the paper. We first explain panel (a). The qubits are the edge qubits of a planar lattice. Each face supports a plaquette stabilizer, which is the product of Z on the four edges around that face.

$$B_p^Z := \prod_{e \in \partial p} Z_e \quad (5)$$

Each vertex supports a star stabilizer, which is the product of X on the four edges that meet at that vertex.

$$A_v^X := \prod_{e \in \nu} X_e \quad (6)$$

The code space \mathcal{C} is the simultaneous $+1$ eigenspace of all stabilizers that are kept active. We write $P_{\mathcal{C}}$ for the projector onto this code space.

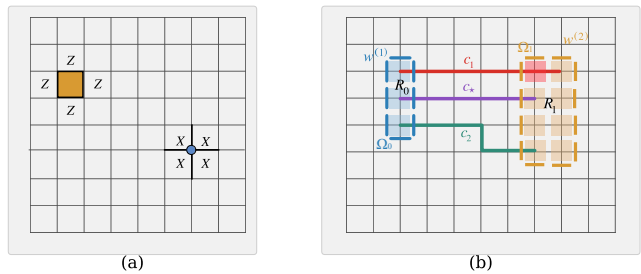


FIG. 1. A planar-code dictionary and the simple example used throughout this work. Panel (a) shows the local stabilizer structure. Data qubits live on edges. For each face, the plaquette check is the product of Z operators on the four surrounding edges. For each vertex, the star check is the product of X operators on the four incident edges. Panel (b) shows a thin planar patch with two rough holes R_0 and R_1 . Equivalently, these are two connected regions where the corresponding star checks are turned off. The dual loops $w^{(1)}$ and $w^{(2)}$ play the role of witnesses. They enclose the witness-guided regions Ω_0 and Ω_1 . In this example, $\Omega_0 = R_0$, while $R_1 \subseteq \Omega_1$. The primal strings c_1 , c_* , and c_2 support the Z -string operators $Z(c_1)$, $Z(c_*)$, and $Z(c_2)$. The X -products supported on the witnesses have the geometry of logical \bar{X} strings. In this example, each compatible signal string crosses the relevant witness with odd parity. This is the geometric pattern behind the common logical \bar{Z} action proved later.

We now explain panel (b). The shaded blue region is the rough hole R_0 , and the shaded orange region is the rough hole R_1 . This is the geometric picture used throughout the main text. Equivalently, each rough hole may be viewed as a connected region where the star checks are turned off. We mention this equivalent stabilizer description only to connect with the standard code construction.

The two rough holes change which Z strings can act as logical operators. After they are introduced, a primal Z path is allowed to start on R_0 and end on R_1 . Such a path is a candidate logical \bar{Z} operator. This is why the three colored primal strings c_1 , c_* , and c_2 are drawn as curves connecting the two rough holes.

At this point it is useful to separate *support* from *operator*. In the main text, a signal support c is a simple primal path of edge qubits. It is a geometric object first. The corresponding operator is

$$Z(c) := \prod_{e \in c} Z_e. \quad (7)$$

Thus the red, purple, and green curves in panel (b) are first path supports, and then, after we attach Z operators to their edges, they become the physical operators $Z(c_1)$, $Z(c_*)$, and $Z(c_2)$.

Next we introduce the concept of witness, which is closely related to the rough holes that define the punctured surface code. First, a witness is a geometric object. It is drawn as a closed, simple loop on the *dual* lattice, namely a closed loop with no repeated vertices along the

way. Here “dual” means that the loop runs through the spaces between the primal vertices and faces, so it crosses primal edges instead of lying on them. Second, the same dual loop defines an operator on the code. If w is such a dual loop, we write

$$X(w) := \prod_{e \in w} X_e, \quad (8)$$

where the product is over all primal edges crossed by w . So a witness is not only a geometric test curve. Its support also carries an X -type string operator. For this reason, it is drawn in the same style as a logical \bar{X} string.

This dual point of view is exactly what we need later. Geometrically, the witness tells us how a primal Z string crosses the patch. On the code, the same witness behaves like an X -type logical support. Later, in the theorem, we will write the same object in algebraic language as a simple closed dual 1-cochain. But at the level of this example, it is enough to think of it as a dual loop that crosses primal edges and supports an X product.

A witness also selects a witness-guided region $\Omega(w)$ by choosing one side of the loop. This region serves only as a geometric guide. The actual rough hole is later chosen as a clean connected subregion $R \subseteq \Omega(w)$. It is chosen so that the assigned signal endpoints lie on the rough boundary, while the interiors of all prescribed signal paths remain in the active code region.

We can now read panel (b) in a simple way. The three primal strings c_1 , c_\star , and c_2 have different microscopic shapes. The red string c_1 takes an upper route. The purple string c_\star is the direct reference path. The green string c_2 takes a lower route before entering the right rough hole. So the figure already shows that the logical action does not depend on one special path in real space.

The two dual loops $w^{(1)}$ and $w^{(2)}$ are the witnesses for the left and right rough holes. Each compatible primal string crosses each relevant witness once modulo 2. This odd crossing is the key visual fact. It means that, although the three strings look different microscopically, they play the same topological role in the patch. After the rough holes are fixed, they act as the same logical \bar{Z} on the code space, up to stabilizers.

The witness itself is not unique. It may be deformed on the dual lattice as long as its parity of crossings with the signal strings does not change. This is the topological content that the later theorem makes precise.

For the main text, we use one fixed geometric model throughout. Each signal support c_α is a simple primal path. This is the clearest physical picture and it is sufficient for the sensing protocol and for Theorem 1. When we later switch to algebraic language in the Supplemental Material, the same object is written as a 1-chain whose support is that path. At this stage, however, the figure serves only as a geometric guide. It tells us what kind of logical compression we want. In the next section, we explain the distributed sensing protocol that uses such a compatible family of logical \bar{Z} strings.

III. DISTRIBUTED SENSING PROTOCOLS

Before stating the topological criterion, we explain the sensing protocol that it supports. This is the surface-code version of weighted-sum sensing in a quantum sensor network.

We now briefly explain why this surface-code construction corresponds to the same sensing task as the standard optimal protocol for a chosen linear functional in distributed quantum sensing [2]. The only difference is the encoding. In the usual network picture, the phase is stored in a nonlocal probe state, such as a GHZ state. Here, the same phase is stored in a single logical qubit of the surface code. Moreover, as long as syndrome extraction and decoding are accurate and fast enough during sensing, correctable errors do not erase the accumulated logical phase. This includes both low-weight incoherent Pauli errors that are correctable by the punctured surface code and additional coherent error terms in the Hamiltonian that are not nontrivial logical operators.

We first fix the normalization of the target coefficients. As in the standard network setting, we write the target linear functional as

$$q = \sum_{\alpha} s_{\alpha} \lambda_{\alpha}, \quad |s_{\alpha}| \leq 1 \text{ for all } \alpha, \quad \max_{\alpha} |s_{\alpha}| = 1. \quad (9)$$

This normalization simply fixes the scale. If the desired coefficients are \tilde{s}_{α} , we define

$$s_* := \max_{\alpha} |\tilde{s}_{\alpha}|, \quad s_{\alpha} := \frac{\tilde{s}_{\alpha}}{s_*}, \quad q := \sum_{\alpha} s_{\alpha} \lambda_{\alpha}. \quad (10)$$

Then the original target is recovered by a known rescaling,

$$\tilde{q} = \sum_{\alpha} \tilde{s}_{\alpha} \lambda_{\alpha} = s_* q. \quad (11)$$

With this convention, the effective logical time t is the time entering the logical Ramsey phase. It is compared against the normalized functional q , and the final precision statement takes the same form as in the sensor-network Heisenberg bound. When a concrete implementation is specified, we distinguish this effective logical time from the actual dwell time of the schedule. We denote the latter by T_{par} for parallel loading and by T_{seq} for sequential hole motion. These times only count intervals during which signal phase is accumulated. They do not include additional overheads from control operations, hole motion, or stabilizer updates.

We assume that the planar patch already carries two rough holes R_0 and R_1 , so that one logical qubit is encoded. We write its logical Pauli operators as \bar{X} and \bar{Z} , and we denote the code space by \mathcal{C} , with projector $P_{\mathcal{C}}$.

We also assume that we are given a family of legal Z -type paths $\{c_{\alpha}\}$ such that each path c_{α} is a simple primal path from R_0 to R_1 , and each operator $Z(c_{\alpha})$ acts as the same logical operator \bar{Z} on \mathcal{C} . In other words, the

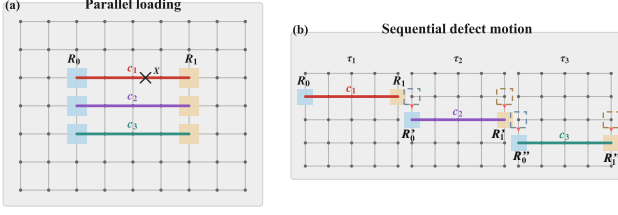


FIG. 2. (a) *Parallel loading*. The rough holes R_0 and R_1 are fixed. Several legal chains c_1, c_2, c_3 are active on the same logical qubit. The mark X denotes a local X flip on an edge qubit along the support. (b) *Sequential hole motion*. The sensing process is divided into three intervals, τ_1, τ_2, τ_3 . During dwell time τ_1 , the active rough holes are R_i , with $i = 0, 1$. At the end of τ_1 , local measurements change the active holes from R_i to R'_i . During dwell time τ_2 , the active rough holes are R'_i . At the end of τ_2 , local measurements change the active holes from R'_i to R''_i . During dwell time τ_3 , the active rough holes are R''_i . Thus the same pair of rough holes follows the sequence $R_i \rightarrow R'_i \rightarrow R''_i$ over the three intervals. During each interval, only one legal Z chain is active. Between intervals, local measurements are performed to move the holes and update the stabilizers, as in SUP1. These updates preserve the encoded logical qubit. Therefore, they do not erase the logical phase accumulated in the previous intervals. In both panels, the total phase is written onto the same logical operator \bar{Z} . The protocol ends with one logical \bar{X} measurement.

physical signal strings may look different in real space, but they all write phase onto the same logical degree of freedom. Theorem 1 and Proposition 2 in the next section tell us when such a compatible family exists. Here we first explain what the protocol does once this compatibility is available.

Proposition 1 (Surface-code weighted-sum sensing). *Assume that each legal signal chain c_α acts as the same logical operator \bar{Z} on the code space \mathcal{C} . Then the normalized target*

$$q = \sum_{\alpha} s_{\alpha} \lambda_{\alpha} \quad (12)$$

can be estimated by a logical Ramsey experiment. Here t is the effective logical time, while T is the dwell time used by the chosen schedule. On the code space, this schedule implements

$$U_{\log}(T) = \exp\left(-\frac{it}{2} \sum_{\alpha} s_{\alpha} \lambda_{\alpha} \bar{Z}\right). \quad (13)$$

The coefficients s_{α} are set by control. They can be programmed either by parallel loading with time-averaged echo control, or by sequential hole motion with chosen dwell times.

The protocol has four simple steps.

1. *Input state*. We prepare the logical $+1$ eigenstate of \bar{X} ,

$$|+_{\bar{L}}\rangle = \frac{1}{\sqrt{2}}(|0_{\bar{L}}\rangle + |1_{\bar{L}}\rangle). \quad (14)$$

This is the logical version of the usual Ramsey input state. It is most sensitive to a phase generated by \bar{Z} .

2. *Sensing evolution*. During the sensing window, the unknown couplings act through physical operators $Z(c_{\alpha})$. Because all active chains represent the same logical operator \bar{Z} , the full physical evolution reduces to one logical Z rotation.

Let $\eta_{\alpha}(t')$ denote the signed activation profile of the α -th signal during $0 \leq t' \leq T$. We use a bang-bang profile,

$$\eta_{\alpha}(t') \in \{-1, 0, +1\}. \quad (15)$$

Here $\eta_{\alpha}(t') = +1$ means that the signal is active with its original sign. The value $\eta_{\alpha}(t') = -1$ means that its sign is reversed by an echo operation. The value $\eta_{\alpha}(t') = 0$ means that the signal is not active during that part of the schedule. General real weights are obtained by changing the duty cycle of this profile.

In the common logical frame, the effective logical Hamiltonian is

$$H_{\log}(t') = \frac{1}{2} \left(\sum_{\alpha} \eta_{\alpha}(t') \lambda_{\alpha} \right) \bar{Z}. \quad (16)$$

Since this Hamiltonian is always proportional to the same logical operator \bar{Z} , the phases add directly. Thus the logical evolution generated during the sensing part of the schedule is

$$U_{\log}(T) = \exp\left[-\frac{i}{2} \left(\sum_{\alpha} \lambda_{\alpha} \int_0^T \eta_{\alpha}(t') dt' \right) \bar{Z}\right]. \quad (17)$$

The schedule realizes the effective evolution in Eq. (13) if

$$\int_0^T \eta_{\alpha}(t') dt' = t s_{\alpha} \quad (18)$$

for every α . Here t is the effective logical time in Eq. (13), while T is the actual dwell time used for sensing. When this condition holds,

$$U_{\log}(T) = \exp\left(-\frac{it}{2} \sum_{\alpha} s_{\alpha} \lambda_{\alpha} \bar{Z}\right). \quad (19)$$

There are two natural ways to realize these coefficients.

Parallel loading. We keep the rough regions R_0 and R_1 fixed. We assume each legal chain c_{α} has at least one chain-specific vertex that is not shared by other chains, so that the X gate control described below applies. Several signal chains may contribute during the same sensing window. A convenient model is

$$H_{\text{par}}(t') = \frac{1}{2} \sum_{\alpha} \eta_{\alpha}(t') \lambda_{\alpha} Z(c_{\alpha}), \quad \eta_{\alpha}(t') \in \{\pm 1\}. \quad (20)$$

To realize the effective evolution in Eq. (13) with effective logical time t , the control must satisfy Eq. (18) for every α . Since $|\eta_{\alpha}(t')| \leq 1$, this requires

$$T_{\text{par}} \geq t \max_{\alpha} |s_{\alpha}|. \quad (21)$$

With our normalization $\max_{\alpha} |s_{\alpha}| = 1$, the minimum parallel dwell time is $T_{\text{par}}^{\text{min}} = t$.

A negative sign is obtained by applying an odd number of local X gates to edge qubits on the support of c_{α} . This echo operation flips

$$Z(c_{\alpha}) \mapsto -Z(c_{\alpha}) \quad (22)$$

during that time segment. These echo controls are treated as known fast control pulses. Any stabilizer sign changes caused by these pulses are tracked in the Pauli frame, so they do not act as unknown physical Pauli errors. Thus the control produces a signed activation profile for each signal. A coefficient with $0 < |s_{\alpha}| < 1$ is obtained from the time average of this signed activation profile. For example, when $T_{\text{par}} = t$, one may take $\eta_{\alpha}(t') = +1$ for a fraction $(1 + s_{\alpha})/2$ of the time and $\eta_{\alpha}(t') = -1$ for a fraction $(1 - s_{\alpha})/2$ of the time. This gives $\int_0^{T_{\text{par}}} \eta_{\alpha}(t') dt' = t s_{\alpha}$. If multiple identical signals acting on the same chain c_{α} are available, multiplicity can also be used. In particular, multiplicity alone is enough for integer and rational weights, while partial-time activation gives a direct route to general normalized real weights.

Sequential hole motion. Instead of keeping all signal chains active on one fixed patch, we may move rough holes through a sequence of nearby positions. For the simple schedule below, we impose a separation condition. At each dwell step, the chosen rough-hole positions make only the intended signal support legal. Chains with the same endpoints are treated as one parallel group with a common weight, unless additional local echo controls distinguish them. At step r , one legal chain c_r is active for a dwell time τ_r . If that step senses the coupling λ_{α_r} , then its contribution is

$$H_r = \frac{1}{2} \sigma_r \lambda_{\alpha_r} Z(c_r), \quad \sigma_r \in \{\pm 1\}, \quad (23)$$

where σ_r records whether an echo is used to reverse the sign in that step.

Let

$$T_{\text{seq}} = \sum_r \tau_r \quad (24)$$

be the actual dwell time of the sequential sensing schedule. To realize the effective evolution in Eq. (13) with effective logical time t , the dwell times must satisfy

$$\sum_{r: \alpha_r = \alpha} \sigma_r \tau_r = t s_{\alpha} \quad (25)$$

for every α . So in the sequential picture, the weights are set by dwell times. The hole motion selects which physical chain is active at each moment, but the phase is always written onto the same logical operator \bar{Z} .

For a fixed α , we choose the dwell time assigned to sense λ_{α} to be $\tau_{\alpha} = t |s_{\alpha}|$, with $\sigma_{\alpha} = \text{sign}(s_{\alpha})$. Hence their total duration is at least $t |s_{\alpha}|$. Therefore,

$$T_{\text{seq}}^{\text{min}} = t \sum_{\alpha} |s_{\alpha}|. \quad (26)$$

Under the normalization $\max_{\alpha} |s_{\alpha}| = 1$, sequential hole motion is therefore generally slower than parallel loading. The slowdown factor is $\sum_{\alpha} |s_{\alpha}|$. This factor can be close to one when the target is dominated by one coefficient. For example, if $|s_{\alpha_0}| = 1$ and $\sum_{\alpha \neq \alpha_0} |s_{\alpha}| \ll 1$, then $T_{\text{seq}}^{\text{min}} \approx t$, so the sequential and parallel schedules have nearly the same dwell time.

Between two dwell periods, we may update the code by local Pauli measurements that move the holes, as described in SUP1. These intermediate code projections change the active stabilizers, but they preserve the encoded logical qubit up to a known Pauli-frame update. Therefore, they do not erase the logical phase already accumulated in the earlier steps. At each step, the active chain still represents the same logical operator \bar{Z} on the instantaneous code space. The phases from all steps therefore add coherently, and the protocol ends with one logical \bar{X} measurement on the final code patch.

We now give a simple example. Suppose the desired quantity is the average of M local couplings,

$$\bar{\lambda} := \frac{1}{M} \sum_{\alpha=1}^M \lambda_{\alpha}. \quad (27)$$

Under our normalization convention, we first sense the normalized sum

$$q_{\text{sum}} := \sum_{\alpha=1}^M \lambda_{\alpha}, \quad s_{\alpha} = 1 \quad \text{for all } \alpha. \quad (28)$$

The average is then obtained by the known rescaling

$$\bar{\lambda} = \frac{q_{\text{sum}}}{M}. \quad (29)$$

In the parallel picture, all M chains can remain active during the same sensing window. Thus q_{sum} is sensed for effective time t using actual dwell time $T_{\text{par}} = t$. In the sequential picture, the chains are visited one by one. Since $s_{\alpha} = 1$ for every α , each chain must dwell for time t . Thus $T_{\text{seq}} = Mt$. Therefore, in this equal-weight example, sequential hole motion realizes the same effective logical evolution as parallel loading, but it takes M times longer. If the actual dwell time is fixed, the sequential protocol has a smaller effective logical time by the same factor.

3. Final measurement. After the schedule realizes the effective logical time t , we measure the logical operator \bar{X} . Starting from $|+L\rangle$, the two outcomes occur with probabilities

$$p_{\pm} = \frac{1}{2} [1 \pm \cos(qt)]. \quad (30)$$

Thus the unknown weighted sum q is read out from one logical Ramsey fringe. This is the same weighted-sum sensing task as in distributed quantum sensing, but now it is encoded in one protected logical qubit.

4. Precision and the average case. As usual for Ramsey metrology, the value of Fisher information reveals the local sensitivity for q -estimation, e.g. when q is known

in advance to be within some small neighborhood of its true value. The binary distribution above has classical Fisher information $F = t^2$. Hence, after ν repetitions, any unbiased estimator Q of the normalized target q satisfies

$$\text{Var}(Q) \geq \frac{1}{\nu t^2}. \quad (31)$$

This is the sensor-network Heisenberg limit for one normalized linear functional.

For the average task, however, it is cleaner to apply this bound to the normalized sensed variable

$$q_{\text{sum}} := \sum_{\alpha=1}^M \lambda_{\alpha}, \quad s_{\alpha} = 1 \quad \text{for all } \alpha, \quad (32)$$

If Q_{sum} is an unbiased estimator of q_{sum} , then

$$\text{Var}(Q_{\text{sum}}) \geq \frac{1}{\nu t^2}. \quad (33)$$

We then estimate the mean by the known rescaling

$$\bar{\Lambda} := \frac{Q_{\text{sum}}}{M}. \quad (34)$$

Therefore,

$$\text{Var}(\bar{\Lambda}) = \frac{\text{Var}(Q_{\text{sum}})}{M^2} \geq \frac{1}{\nu M^2 t^2}. \quad (35)$$

Equivalently,

$$\Delta \bar{\Lambda} \geq \frac{1}{\sqrt{\nu} M t}. \quad (36)$$

Thus, as a function of the effective logical time t , the average case recovers the usual Heisenberg scaling in the number of sensors. For the parallel implementation, this is also the scaling in the actual sensing time because $T_{\text{par}} = t$. For the sequential implementation, the same effective time requires $T_{\text{seq}} = Mt$.

The key difference from the usual GHZ picture is the physical form of the protocol. Here the accumulated phase is stored at the logical level. Therefore, as long as standard surface-code error correction can be carried out sufficiently well during the sensing process, all correctable local errors can be removed without erasing the target phase. The remaining question is geometric: when can a given family of signal chains $\{c_{\alpha}\}$ be made compatible in this sense? Theorem 1 answers exactly that question.

IV. DESIGN RULES WITH DISJOINT SUPPORTS

We now turn to the geometric question behind Proposition 1. We assume each signal support c_{α} is a connected simple primal path of data qubits, and different signals do not share qubits. The question is the following: when

do all operators $Z(c_{\alpha})$ act as the same nontrivial logical \bar{Z} on the code space?

We use the planar-code picture introduced above. The patch carries two rough holes R_0 and R_1 . Equivalently, these holes are the actual connected regions of removed star checks, which are distinct from the auxiliary witness-guided regions Ω_0 and Ω_1 used below. A primal Z string is then allowed to start on R_0 and end on R_1 . Such a string is a candidate logical \bar{Z} operator.

The key object is again the witness. As in Fig. 1, a witness is a loop on the dual lattice. To compare it with a primal string c , we look edge by edge. For each primal edge e , we ask two yes-or-no questions: does c use this edge, and does the simple dual loop w cross this edge? These answers are binary variables, denoted by $c_e, w_e \in \{0, 1\}$. We then define

$$\langle w, c \rangle := \sum_e w_e c_e \pmod{2}. \quad (37)$$

So $\langle w, c \rangle$ is just the parity of the crossings between w and c . If they cross once, or three times, then $\langle w, c \rangle = 1$. If they cross zero, two, or four times, then $\langle w, c \rangle = 0$.

There are two separate questions.

First, there is a global topological question. It asks whether the signal paths admit one common odd witness. This question does not yet involve the actual rough holes. It is answered by the global odd-witness criterion below.

Second, there is a local geometric realization question. It asks whether a common odd witness can be converted into two actual clean rough holes. This question does involve the removed star checks. It depends on whether the proposed hole regions can be opened without turning off star checks at non-terminal vertices of the prescribed signal paths. It is answered by the clean puncture realization statement after the theorem.

A. Odd-witness criterion

We first answer the global question. For each signal path c_{α} , let its endpoints (vertices) be u_{α} and v_{α} . Define the endpoint graph Γ_{end} as follows. The vertices of Γ_{end} are all endpoints that appear among the signal paths. For each c_{α} , we add one abstract edge η_{α} between u_{α} and v_{α} . The edge η_{α} records only the two endpoints of c_{α} . It does not record the geometric shape of c_{α} .

Theorem 1 (Global odd-witness criterion). *Assume the disjoint-support regime. Let $\{c_{\alpha}\}_{\alpha \in \mathcal{I}}$ be simple primal paths on one planar patch, with pairwise disjoint edge supports. Then the following statements are equivalent.*

- (a) *The endpoint graph Γ_{end} is bipartite. Equivalently, every cycle in Γ_{end} has even length.*
- (b) *There is no subset $\mathcal{A} \subseteq \mathcal{I}$ such that $|\mathcal{A}|$ is odd and*

$$D \left(\bigoplus_{\alpha \in \mathcal{A}} c_{\alpha} \right) = 0. \quad (38)$$

(c) There exists a simple closed dual witness w such that

$$\langle w, c_\alpha \rangle = 1 \quad \text{for all } \alpha \in \mathcal{I}. \quad (39)$$

Condition (a) says that the endpoint vertices of the signal paths can be colored with two colors in such a way that every signal path connects vertices of opposite colors. Equivalently, Γ_{end} contains no odd cycle. In condition (b), D is an endpoint-parity map. Given a collection of paths, D lists all their endpoint vertices and cancels identical vertices in pairs. Thus D returns precisely those endpoint vertices that occur with odd multiplicity. Therefore, the equation in condition (b) says that the paths indexed by \mathcal{A} have no unpaired endpoints; equivalently, every endpoint vertex appears an even number of times. In terms of Γ_{end} , this means that each endpoint vertex is incident to an even number of the selected paths. Condition (b) rules out the possibility that such complete endpoint cancellation occurs for an odd number of selected paths. This is exactly the obstruction given by an odd cycle, and hence is equivalent to the bipartiteness of Γ_{end} . Condition (c) says that every signal path crosses the same simple closed dual loop with odd parity.

For example, the paths do not share endpoint vertices in Fig. 3, and the endpoint graph is a disjoint union of edges and is bipartite by default, satisfying condition (a) and an odd witness can then be found by Theorem 1. In Fig. 4, we provide an example where the paths share endpoint vertices. Note that even though the supports of paths are disjoint, their endpoint vertices may still coincide. In this case, the existence of an odd witness depends on whether the endpoint graph contains an odd cycle. Even cycles like Fig. 4 are allowed, whereas odd cycles are the obstruction. Fig. 4 provides an example where the global condition for finding the rough holes (Theorem 1) is satisfied, but the local condition (Proposition 2) is not. We will discuss this situation later in detail.

The Supplemental Material proves the algebraic form first, where the witness is a closed dual 1-cochain. It then shows that, for the present planar setting, one may choose a simple closed representative without changing the odd parities in Eq. (39).

Theorem 1 is about global topology. It does not yet provide a construction of the rough holes for us. It only says when the signal family admits one common odd witness.

B. Cleanly openable regions

We now turn to the second, local question. Choose a simple odd-witness representative $w^{(1)}$. Because $w^{(1)}$ crosses every signal path c_α with odd parity, the two endpoints of c_α lie on opposite sides of $w^{(1)}$. Choose one side as the first witness-guided region Ω_0 . The endpoints on this side are the endpoints that will terminate on the first rough hole R_0 —a region within Ω_0 to be found later.

The other endpoints will terminate on the second rough hole R_1 .

The region Ω_0 is only a guide. It is not itself a rough hole. After R_0 has been fixed, a second odd-witness representative $w^{(2)}$ will guide the choice of Ω_1 . Thus Ω_0 and Ω_1 need not come from the same witness representative. In particular, Ω_i is only a witness-guided candidate region, while R_i is the actual hole used in the code.

Note that a signal path is allowed to pass through a witness-guided region Ω_i . This does not by itself cause a problem. When the actual rough hole R_i is chosen, the non-terminal parts of the prescribed signal paths are simply excluded from R_i —to guarantee c_α act as logical operators in the punctured surface code. Here the non-terminal parts of a prescribed simple path c_α are the star-check vertices where the path passes through rather than ends. Equivalently, such a vertex is touched by two edges within c_α . The only local requirement we will need is that, after this exclusion, one can still choose a connected rough hole with the required endpoint contacts.

We say that the witness-guided regions are *cleanly openable* if one can choose two disjoint connected actual rough holes $R_0 \subseteq \Omega_0$ and $R_1 \subseteq \Omega_1$ satisfying the following two conditions. First, each prescribed signal path c_α has one endpoint on the rough boundary of R_0 and the other endpoint on the rough boundary of R_1 . Second, the non-terminal part of every prescribed signal path c_α remains in the active code region (outside $R_{0,1}$). Equivalently, when the actual rough holes are chosen, no star check at a non-terminal vertex of any c_α is turned off.

Proposition 2 (Clean puncture realization). *Assume the global odd-witness condition holds. Assume further that the two-stage construction described above is cleanly openable. Let $R_0 \subseteq \Omega_0$ and $R_1 \subseteq \Omega_1$ be the resulting clean actual rough holes.*

Then each signal path c_α has one endpoint on the rough boundary of R_0 and the other endpoint on the rough boundary of R_1 , while its non-terminal part remains in the active code region.

Let c_\star be any fixed primal path with one endpoint on the rough boundary of R_0 and the other endpoint on the rough boundary of R_1 , whose non-terminal part also remains in the active code region. For fixed clean rough holes, any two such paths differ only by products of Z -type plaquette stabilizers. Hence all prescribed signal paths have the same code-space action as c_\star :

$$P_C Z(c_\alpha) P_C = P_C Z(c_\star) P_C \neq 0 \quad \text{for all } \alpha. \quad (40)$$

Thus all prescribed signal operators $Z(c_\alpha)$ realize the same nontrivial logical operator \bar{Z} , represented for example by $Z(c_\star)$.

Conversely, suppose two clean actual rough holes R_0 and R_1 are already fixed in the two-hole planar setting considered here. If every prescribed signal path c_α has one endpoint on the rough boundary of R_0 and the other endpoint on the rough boundary of R_1 , with its non-terminal part in the active code region, then there is a

simple closed dual witness w separating R_0 from R_1 . Every such signal path crosses this separator with odd parity. Hence

$$\langle w, c_\alpha \rangle = 1 \quad \text{for all } \alpha. \quad (41)$$

Thus the global odd-witness condition is necessary for any fixed clean two-hole realization.

The forward direction says that the global odd-witness condition (Theorem 1) becomes sufficient for the existence of the required punctured surface code, after imposing the local clean-openability condition. The witness gives the global endpoint assignment, while the clean condition checks whether this assignment can be realized by connected actual rough holes. The converse direction is a necessity statement for fixed clean rough holes. Once R_0 and R_1 are fixed, any prescribed signal path connecting their rough boundaries must cross a dual separator between the two holes with odd parity.

The witness and the logical Z string obey different boundary rules. The witness is closed in the dual sense: it has no endpoints on the dual lattice. A logical Z string is different. After the rough holes are introduced, a primal Z string may start on the rough boundary of R_0 and end on the rough boundary of R_1 . It is therefore not an ordinary closed primal cycle. It is a relative cycle for the punctured patch. Its endpoints are allowed because the corresponding star checks are turned off on the rough holes.

For readers who want the algebraic, the closedness of the witness is written in the Supplemental Material as

$$B^T w = 0, \quad (42)$$

where B is the face-edge incidence matrix over \mathbb{F}_2 . This formula only says that the dual support of w has no endpoints: around each plaquette, the loop enters and leaves in pairs. Likewise, saying that two primal strings differ only by plaquette stabilizers means that their supports differ by a sum of plaquette boundaries. We keep that algebraic language mostly in the Supplemental Material. In the main text, the geometric picture is the more useful one.

If no global odd witness satisfying Eq. (39) exists, then the prescribed signal family cannot be realized as one common logical operator by this clean two-hole construction. In that case, the family must be modified, split into smaller compatible groups, or treated by another control strategy.

C. Constructing the punctured surface code

The global odd-witness criterion is not only a test. Together with the local clean rule, it gives a concrete construction. Figure 3 shows the construction.

We first state the clean-up rule used in the construction.

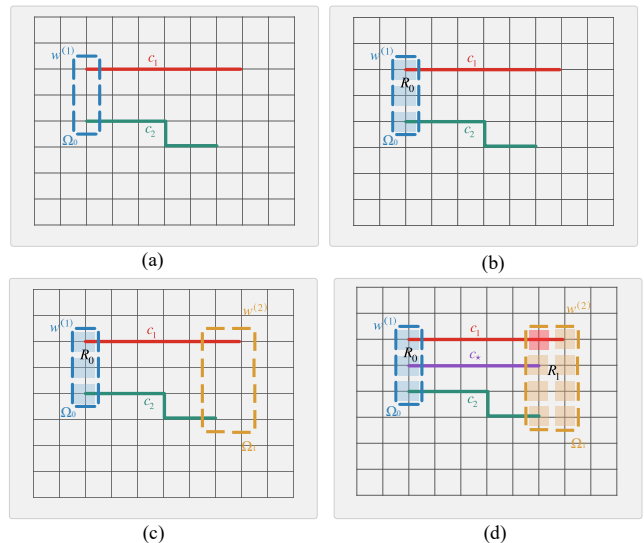


FIG. 3. Stepwise synthesis of two clean rough holes from a global odd witness and the local clean rule. Panel (a) shows a first simple odd-witness representative $w^{(1)}$. It has odd parity with all compatible signal strings and guides the choice of Ω_0 . Panel (b) opens the first actual rough hole $R_0 \subseteq \Omega_0$. Only selected star checks in R_0 are turned off. Panel (c) chooses a second simple odd-witness representative $w^{(2)}$ on the side away from R_0 . It guides the choice of Ω_1 . Panel (d) opens the second actual rough hole $R_1 \subseteq \Omega_1$ and shows a reference string c_\star . Here R_1 is strictly smaller than Ω_1 because a non-terminal part of c_1 passes through Ω_1 . This part is excluded from the actual rough hole and remains in the active code region. The remaining hole-opening region is still connected, so the clean-opening condition is satisfied. After this local cleanup, the clean realization proposition applies. Hence all compatible signal strings act as the same nontrivial logical \bar{Z} .

Clean-up rule. Given a witness-guided region Ω_i , we choose the actual rough hole as a connected subregion $R_i \subseteq \Omega_i$, specified by the star checks to be turned off in the punctured surface code. The region R_i must include the star checks at the assigned endpoint vertices, so that these endpoints lie on the rough boundary. It must also exclude the non-terminal parts of all prescribed signal paths. Equivalently, along a prescribed signal path, only the star checks at the assigned endpoint vertices may be turned off; all non-terminal vertices remain in the active code region. Note that the existence of $R_{0,1}$ satisfying the above conditions is guaranteed when $\Omega_{0,1}$ are cleanly openable.

A signal path may therefore pass through Ω_i . This is harmless, because its non-terminal portion is carved out when R_i is chosen. In practice, one may start from Ω_i as the candidate hole-opening region, then carve out any non-terminal parts of the prescribed signal paths and keep them in the active code region. The clean-up succeeds if the remaining region still contains the assigned endpoints and can be chosen connected as the actual rough hole R_i .

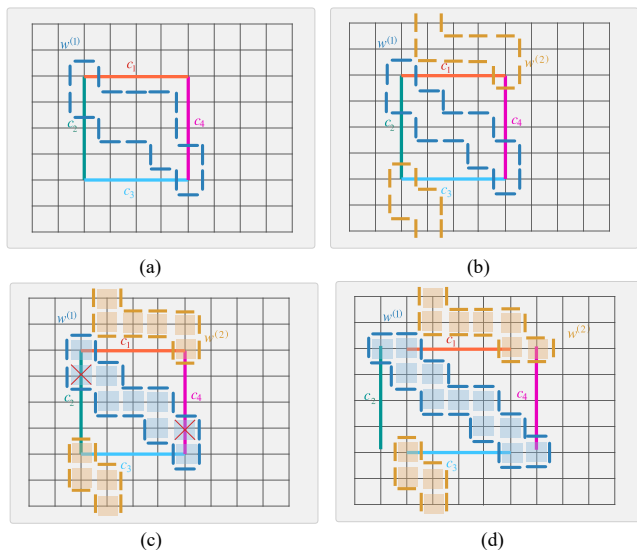


FIG. 4. A local obstruction to the clean realization step, and a simple local repair. The top and bottom edges look connected only because the figure shows a small part of a larger planar patch. The code geometry used in this work is still an ordinary planar patch, not a torus. (a) The first odd-witness representative $w^{(1)}$ crosses each of the four signal paths c_1, c_2, c_3, c_4 exactly once. (b) A second odd-witness representative $w^{(2)}$ can also be chosen so that it crosses each signal path exactly once. Thus the global odd-witness criterion is satisfied. (c) Even so, the clean rough-hole construction can fail locally. The shaded regions indicate the intended hole-opening regions. Some non-terminal parts of the signal paths, indicated by the marked site, lie inside the intended hole-opening regions. They cannot be included in the actual rough holes. Only endpoint contacts with the rough boundary are allowed, and the rest of each signal path must remain in the active code region. After these non-terminal parts are excluded, the remaining candidate region is disconnected. Thus no connected clean rough hole can be chosen in panel (c). (d) This obstruction is not fundamental. If c_2 and c_4 are shifted by one column, while c_1 and c_3 are kept unchanged, the same global pattern becomes compatible with the clean rough-hole construction. This shows that the failure in panel (c) is caused by a local layout issue, not by a global topological obstruction.

We now describe the construction.

- (1) By Theorem 1, choose a simple odd-witness representative $w^{(1)}$. Choose one side of $w^{(1)}$ as the first witness-guided region Ω_0 . The endpoints on this side are assigned to the first rough hole. The other endpoints are assigned to the second rough hole. The region Ω_0 is only a guide, not the actual rough hole.

A shorter representative may be used to keep the construction local, but this choice does not change the topological criterion.

- (2) Apply the clean-up rule inside Ω_0 to the endpoints assigned to the first rough hole. This gives a connected actual rough hole $R_0 \subseteq \Omega_0$. The rough

boundary of R_0 contains these assigned endpoints, while the non-terminal parts of all prescribed signal paths remain in the active code region.

- (3) Keep R_0 fixed and collapse it to one rough vertex \hat{r}_0 . After this collapse, each signal path has one endpoint at \hat{r}_0 and one remaining endpoint outside R_0 . Thus the quotient endpoint graph is a star graph, possibly with repeated edges, and is therefore bipartite.

Apply Theorem 1 to this quotient patch. This gives a second simple odd-witness representative $w^{(2)}$. Lift it back to the original patch. Let Ω_1 be the side of $w^{(2)}$ that contains the remaining endpoints and does not contain R_0 .

- (4) Apply the same clean-up rule inside Ω_1 to the remaining endpoints. This gives a connected actual rough hole $R_1 \subseteq \Omega_1$. The rough boundary of R_1 contains the remaining endpoints, while the non-terminal parts of all prescribed signal paths remain in the active code region.

Panels (a)–(d) of Fig. 3 follow these four steps: first $w^{(1)}$, then Ω_0 and R_0 , then $w^{(2)}$, and finally Ω_1 and R_1 together with the reference path c_* . The full proof is given in the Supplemental Material.

Figure 4 explains why the clean realization step needs a separate local check. The odd-witness condition is global. It may hold even when the local layout near a planned hole is too crowded. In that case, the theorem still gives odd-witness representatives and witness-guided regions Ω_0 and Ω_1 . However, there may be no clean actual rough holes $R_0 \subseteq \Omega_0, R_1 \subseteq \Omega_1$. This obstruction is purely local. It occurs when the intended hole-opening region contains non-terminal parts of the prescribed signal paths. These non-terminal parts cannot be included in the actual rough hole, because the clean construction allows only endpoint contacts with the rough boundary. The rest of each signal path must remain in the active code region. If excluding these non-terminal parts disconnects the remaining candidate region, then no connected clean rough hole can be chosen. This is not a failure of the global odd-witness criterion. It is a failure of the local clean realization step. It can often be removed by a small local deformation of the signal paths, as shown in panel (d).

Together, Proposition 1, Theorem 1, and Proposition 2 give the full strategy to perform distributed sensing for Z -type couplings with disjoint supports. Proposition 1 gives the sensing protocol once all signal operators act as the same logical \bar{Z} . Theorem 1 gives the global parity test. Proposition 2 gives the local condition that turns the witness-guided regions into actual clean rough holes. Under these two conditions, the disjoint signal family is compressed into one protected logical generator.

V. DESIGN RULES WITH OVERLAPPING SUPPORTS

We now turn to overlapping supports and ask when a punctured surface code can still be used.

In the disjoint-support regime, the supports $\{c_\alpha\}$ are fixed in advance and are pairwise disjoint. The question is then the same as before: do all operators $Z(c_\alpha)$ act as the same nontrivial logical \bar{Z} on the code space? If overlaps are allowed, the question changes. We must now answer two questions. First, which overlapping three-body signal terms are still compatible with our common logical- \bar{Z} sensing protocol? Second, if they are compatible, how should they be placed on the planar patch? In this section we study the simplest nontrivial case, namely overlapping three-body Z signals.

As before, each support c_α is a connected simple primal path of data-qubit edges. We keep the same notation: c_α denotes the support, and $Z(c_\alpha)$ denotes the corresponding physical operator. Here we further impose $|c_\alpha| = 3$ for every α . So each signal chain is a connected three-edge primal path, and each signal operator is a three-qubit Z string.

A simple example shows the setting. Suppose

$$Z(c_1) = Z_{q_1}Z_{q_2}Z_{q_3}, \quad Z(c_2) = Z_{q_3}Z_{q_4}Z_{q_5}, \quad (43)$$

so the two three-body terms share one data qubit. The question is whether, after introducing the rough holes R_0 and R_1 , both $Z(c_1)$ and $Z(c_2)$ can still act as the same logical \bar{Z} on the code space. If the answer is yes, we must then ask how such overlapping chains can be arranged on the planar patch. Figure 5 shows that even this simplest type of overlap is already highly constrained. The purpose of this section is to state those compatibility and placement rules explicitly.

Our goal is to identify all possible patterns for three-body Hamiltonian estimation that involves overlapping support where our punctured surface code approach applies. All operators $Z(c_\alpha)$ must act in the same way on the code space. Equivalently, they must all represent the same logical \bar{Z} . This requirement gives one hard algebraic constraint, proved in SUP6.

Rule 1: two distinct three-body Z -signal chains may share at most one data qubit. Indeed, if two distinct three-body chains shared two data qubits, then the product of the two corresponding operators would have weight two. But a nontrivial weight-two Z operator flips at least one star check. So it cannot be a surface-code stabilizer. Hence such a pair is not compatible.

After Rule 1, the remaining restrictions are geometric. So the compatibility check is naturally stepwise: we first apply Rule 1 to exclude forbidden pairwise overlaps, then apply Rules 2 and 3 to fix the long-range backbone pattern, and finally apply Rule 4 to determine the allowed endpoint-local completion. Figure 5 shows the picture we need. In one connected cluster of overlapping three-body chains, the successive one-qubit overlaps can line up into one long pattern across the patch. We call this long red

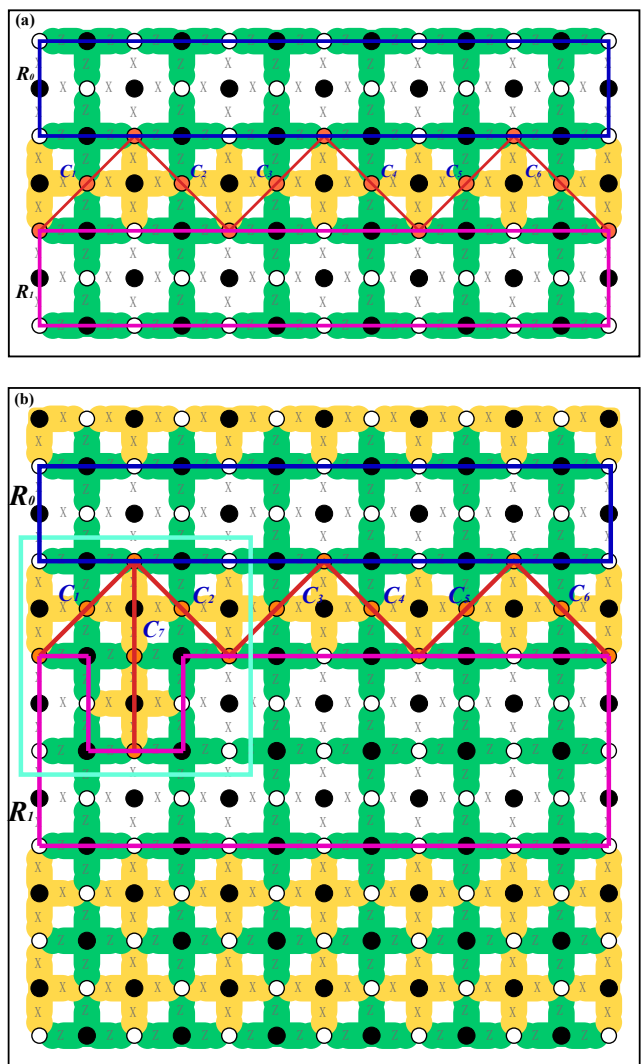


FIG. 5. **Compatible placement of overlapping three-body Z -signal chains on punctured surface code lattice.** White circles denote data qubits, and black circles denote syndrome-measurement qubits. The green regions carry Z -type stabilizers, and the yellow regions carry X -type stabilizers. Each (red) labeled chain C_i denotes a support c_i , namely a connected three-edge primal path on data qubits. The corresponding physical signal operator is $Z(c_i)$. The (blue and pink) boxes R_0 and R_1 mark the two rough holes, that is, the two connected regions where the relevant X -type checks are turned off. (a) Basic compatible skeleton. The red polyline is the long overlap backbone. It is a single open path. The displayed chains C_1, \dots, C_6 show the basic long-range placement pattern that is compatible with one common logical \bar{Z} action on the code space. (b) Allowed local completion of the same skeleton. The cyan box shows an allowed endpoint-local patch near the left endpoint. It represents the allowed local completion of this type. This patch inserts the additional chain C_7 between C_1 and C_2 . Here C_1 , C_2 , and C_7 meet at one data qubit, but the junction stays local. It does not create a second long backbone, and it does not close the backbone into a loop.

pattern the *backbone*. If this red pattern splits into two long directions, we say that the backbone branches.

For the three-body layouts of Fig. 5, compatibility and placement give three more rules.

Rule 2: the backbone must not branch. So a compatible cluster must be placed along one long backbone only. Equivalently, the allowed three-body signals must line up as one open chain of successive one-qubit overlaps, for example

$$Z_{q_1}Z_{q_2}Z_{q_3} \longrightarrow Z_{q_3}Z_{q_4}Z_{q_5} \longrightarrow Z_{q_5}Z_{q_6}Z_{q_7} \longrightarrow \dots \quad (44)$$

Each arrow means that two neighboring terms share exactly one data qubit. By contrast, a pattern such as

$$\begin{array}{c} Z_{q_1}Z_{q_2}Z_{q_3} \longrightarrow Z_{q_3}Z_{q_4}Z_{q_5} \longrightarrow Z_{q_5}Z_{q_6}Z_{q_7}, \\ \searrow \\ Z_{q_3}Z_{q_8}Z_{q_9} \longrightarrow Z_{q_9}Z_{q_{10}}Z_{q_{11}}, \end{array} \quad (45)$$

is not allowed, because the overlap pattern splits into two directions at the shared qubit q_3 . Such a branch is not compatible with one common logical \bar{Z} action.

Rule 3: the backbone must not close into a loop. In other words, if we follow the successive one-qubit overlaps from one support to the next, we must not come back to the support where we started. So the allowed pattern is an open chain of signals, not a cyclic one. For example, a cyclic pattern of the form

$$\begin{array}{c} Z_{q_1}Z_{q_2}Z_{q_3} \longrightarrow Z_{q_3}Z_{q_4}Z_{q_5} \longrightarrow Z_{q_5}Z_{q_6}Z_{q_7} \longrightarrow \dots \\ \longrightarrow Z_{q_{n-1}}Z_{q_n}Z_{q_1} \longrightarrow Z_{q_1}Z_{q_2}Z_{q_3} \end{array} \quad (46)$$

is not allowed. The long red backbone must therefore stay open. Here “loop” refers only to this overlap pattern among the supports.

Rule 4: apart from the open backbone itself, the only extra feature allowed is an endpoint-local patch of the type shown in Fig. 5(b). So, once a compatible backbone is fixed, any extra placement must remain a local endpoint modification of this kind.

In operator language, one first places the main open chain

$$Z_{q_1}Z_{q_2}Z_{q_3} \longrightarrow Z_{q_3}Z_{q_4}Z_{q_5} \longrightarrow Z_{q_5}Z_{q_6}Z_{q_7} \longrightarrow \dots \quad (47)$$

Then one may add an extra local term near an endpoint:

$$\begin{array}{c} Z_{q_1}Z_{q_2}Z_{q_3} \longrightarrow Z_{q_3}Z_{q_4}Z_{q_5} \longrightarrow Z_{q_5}Z_{q_6}Z_{q_7} \longrightarrow \dots \\ \uparrow \\ Z_{q_3}Z_{q_8}Z_{q_9}. \end{array} \quad (48)$$

This gives an endpoint-local patch of the allowed type. Its precise local realization may vary, but the key point is the same: it must remain local and cannot be extended further into a longer chain. So it never creates a second long backbone.

Figure 5(a) shows the basic compatible skeleton. The red backbone is a single open path. This is the only

long-range placement pattern without a branch. Along this path, the local overlap pattern alternates from step to step. In other words, as we move from one chain to the next, the overlap switches from one side of the backbone to the other. So the local pattern flips each time. This already rules out an odd loop, because after an odd number of steps we would return to the opposite local arrangement.

For an even loop, parity alone would not be enough if one imposed periodic boundary conditions and treated the two sides as equivalent. That point of view can be useful as a theoretical simplification, but it is not the setting considered here. Here we consider an ordinary planar patch with non-periodic boundaries and two rough regions. The backbone therefore has a definite start, a definite end, and a fixed direction along the patch. Hence it cannot turn around and close on itself.

Figure 5(b) shows an allowed local completion near an endpoint. The cyan box marks this extra local patch. It inserts a short three-body chain between the first two endpoint terms. This creates a local junction, but it stays local. It does not produce a second long backbone. Moreover, this local completion cannot be extended, because the nearby area is already absorbed by the rough region and leaves no room for it to grow into a longer chain.

In summary, this section tells us which three-body overlap patterns are compatible with one common logical \bar{Z} action, and it tells us how such compatible signals must be placed on the planar patch. Rule 1 forbids two-qubit overlaps. Rules 2 and 3 force the compatible pattern to remain a single open backbone. Rule 4 shows that any extra feature must be an endpoint-local patch of the allowed type. Thus every compatible cluster in this setting is an open chain, up to such a local endpoint modification. Further details are given in SUP6.

VI. DISCUSSION

In this paper we study the metrological task of estimating a chosen linear functional of local couplings on a surface-code patch, $q = \sum_{\alpha} s_{\alpha} \lambda_{\alpha}$ for known coefficients s_{α} and unknown coupling strengths λ_{α} . For this task, we give a topological criterion that certifies when many local, disjoint Z -type couplings implement the same non-trivial logical \bar{Z} . Furthermore, the criterion is constructive, where the locations of the holes can be identified for given sets of signal chains. Combined with the logical Ramsey protocol developed in the main text, this converts the physical sensing Hamiltonian into one protected logical generator for the target quantity q . In this sense, the protocol gives a protected realization of weighted-sum sensing in a quantum sensor network. While we focus on Z -type signals for concreteness, the same framework applies to X -type couplings by exchanging X and Z throughout.

For three-body signals with overlapping supports, the allowed placements are more restrictive: two-qubit over-

laps are forbidden, and compatible clusters must follow one open backbone, up to endpoint-local modifications. Even with these caveats, many layouts in this setting still admit a clean logical reduction. Assuming syndrome extraction can be performed accurately and sufficiently fast during sensing, all errors that remain correctable by the code do not erase the accumulated logical phase. Moreover, the phase is stored nonlocally, so an observer restricted to a correctable region cannot recover q from local measurements within that region (SUP5). Future work can extend the same geometric criteria to richer code families, higher-weight interactions, and more general Pauli structure. The Supplemental Material contains

the full proofs, no-go statements, and the detailed construction algorithms.

ACKNOWLEDGEMENTS

L.Q. thanks Haidong Yuan, Jun Feng, and Zhiyao Hu for helpful discussions. S.Z. acknowledges support from Perimeter Institute for Theoretical Physics, a research institute supported in part by the Government of Canada through the Department of Innovation, Science and Economic Development Canada and by the Province of Ontario through the Ministry of Colleges and Universities.

-
- [1] Z. Zhang and Q. Zhuang, Distributed quantum sensing, *Quantum Sci. Technol.* **6**, 043001 (2021), [arXiv:2010.14744 \[quant-ph\]](#).
- [2] Z. Eldredge, M. Foss-Feig, J. A. Gross, S. L. Rolston, and A. V. Gorshkov, Optimal and secure measurement protocols for quantum sensor networks, *Phys. Rev. A* **97**, 042337 (2018), [arXiv:1607.04646 \[quant-ph\]](#).
- [3] T. J. Proctor, P. A. Knott, and J. A. Dunningham, *Networked quantum sensing* (2017), [arXiv:1702.04271 \[quant-ph\]](#).
- [4] T. J. Proctor, P. A. Knott, and J. A. Dunningham, Multiparameter Estimation in Networked Quantum Sensors, *Phys. Rev. Lett.* **120**, 080501 (2018), [arXiv:1707.06252 \[quant-ph\]](#).
- [5] J. Rubio, P. A. Knott, T. J. Proctor, and J. A. Dunningham, Quantum sensing networks for the estimation of linear functions, *J. Phys. A A* **53**, 344001 (2020), [arXiv:2003.04867 \[quant-ph\]](#).
- [6] Q. Zhuang, Z. Zhang, and J. H. Shapiro, Distributed quantum sensing using continuous-variable multipartite entanglement, *Physical Review A* **97**, 032329 (2018).
- [7] W. Ge, K. Jacobs, Z. Eldredge, A. V. Gorshkov, and M. Foss-Feig, Distributed quantum metrology with linear networks and separable inputs, *Physical review letters* **121**, 043604 (2018).
- [8] J. Bringewatt, I. Boettcher, P. Niroula, P. Bienias, and A. V. Gorshkov, Protocols for estimating multiple functions with quantum sensor networks: Geometry and performance, *Physical Review Research* **3**, 033011 (2021).
- [9] T. Qian, J. Bringewatt, I. Boettcher, P. Bienias, and A. V. Gorshkov, Optimal measurement of field properties with quantum sensor networks, *Physical Review A* **103**, L030601 (2021).
- [10] E. Abbasgholinejad, S. R. Muleady, J. Bringewatt, L. O. Conlon, and A. V. Gorshkov, *Multiparameter function estimation for general hamiltonians* (2026), [arXiv:2605.04136 \[quant-ph\]](#).
- [11] M. A. Nielsen and I. L. Chuang, *Quantum Computation and Quantum Information*, 10th ed. (Cambridge University Press, Cambridge, 2010).
- [12] E. Knill and R. Laflamme, Theory of quantum error-correcting codes, *Phys. Rev. A* **55**, 900 (1997).
- [13] S. Zhou, M. Zhang, J. Preskill, and L. Jiang, Achieving the heisenberg limit in quantum metrology using quantum error correction, *Nature Communications* **9**, 78 (2018).
- [14] E. M. Kessler, I. Lovchinsky, A. O. Sushkov, and M. D. Lukin, Quantum error correction for metrology, *Phys. Rev. Lett.* **112**, 150802 (2014).
- [15] T. Uden, P. Balasubramanian, D. Louzon, Y. Vinkler, M. B. Plenio, M. Markham, D. Twitchen, A. Stacey, I. Lovchinsky, A. O. Sushkov, M. D. Lukin, A. Retzker, B. Naydenov, L. P. McGuinness, and F. Jelezko, Quantum metrology enhanced by repetitive quantum error correction, *Phys. Rev. Lett.* **116**, 230502 (2016).
- [16] S. Zhou and L. Jiang, Asymptotic theory of quantum channel estimation, *PRX Quantum* **2**, 010343 (2021).
- [17] D. Layden, S. Zhou, P. Cappellaro, and L. Jiang, Ancilla-free quantum error correction codes for quantum metrology, *Phys. Rev. Lett.* **122**, 040502 (2019).
- [18] D. Layden and P. Cappellaro, Spatial noise filtering through error correction for quantum sensing, *npj Quantum Information* **4**, 30 (2018).
- [19] H. Chen, Y. Chen, J. Liu, Z. Miao, and H. Yuan, Quantum metrology enhanced by leveraging informative noise with error correction, *Phys. Rev. Lett.* **133**, 190801 (2024).
- [20] G. Arrad, Y. Vinkler, D. Aharonov, and A. Retzker, Increasing sensing resolution with error correction, *Phys. Rev. Lett.* **112**, 150801 (2014).
- [21] D. Gottesman, Stabilizer codes and quantum error correction (1997), [arXiv:quant-ph/9705052](#).
- [22] S. B. Antu and S. Zhou, Stabilizer codes for heisenberg-limited many-body hamiltonian estimation, *Quantum* **9**, 1766 (2025), [arXiv:2408.11101 \[quant-ph\]](#).
- [23] A. Kitaev, Fault-tolerant quantum computation by anyons, *Annals of Physics* **303**, 2 (2003).
- [24] E. Dennis, A. Kitaev, A. Landahl, and J. Preskill, Topological quantum memory, *Journal of Mathematical Physics* **43**, 4452 (2002).
- [25] A. G. Fowler, M. Mariantoni, J. M. Martinis, and A. N. Cleland, Surface codes: Towards practical large-scale quantum computation, *Phys. Rev. A* **86**, 032324 (2012).
- [26] R. Raussendorf, J. Harrington, and K. Goyal, A fault-tolerant one-way quantum computer, *Annals of Physics* **321**, 2242 (2006).
- [27] D. Horsman, A. G. Fowler, S. Devitt, and R. Van Meter, Surface code quantum computing by lattice surgery, *New Journal of Physics* **14**, 123011 (2012).

- [28] W. Gorecki, S. Zhou, L. Jiang, and R. Demkowicz-Dobrzanski, Optimal probes and error-correction schemes in multi-parameter quantum metrology, [Quantum](#) **4**, 288 (2020), [arXiv:1901.00896 \[quant-ph\]](#).

SUP1 LOGICAL INVARIANCE UNDER STABILIZER UPDATES AND SEQUENTIAL SENSING

We work on an n -qubit Hilbert space. The physical space is $\mathcal{H} = (\mathbb{C}^2)^{\otimes n}$. The n -qubit Pauli group is

$$\mathcal{P}_n = \{\pm 1, \pm i\} \times \{I, X, Y, Z\}^{\otimes n}. \quad (49)$$

A global phase $\pm 1, \pm i$ does not affect measurement statistics, and we often ignore such phases when discussing Pauli representatives and commutation relations. However, when defining the stabilizer group, the signs of stabilizer elements still matter. In particular, we require $-I \notin \mathcal{S}$; otherwise the code space would be empty.

A stabilizer code is defined by an abelian subgroup of \mathcal{P}_n . We write

$$\mathcal{S} = \langle P_1, \dots, P_m \rangle \subset \mathcal{P}_n, \quad (50)$$

where the generators P_i are independent and mutually commuting. We require

$$-I \notin \mathcal{S}. \quad (51)$$

The code space is the joint +1 eigenspace of all generators:

$$\mathcal{C} = \{|\psi\rangle \in \mathcal{H} \mid P_i|\psi\rangle = |\psi\rangle \text{ for all } i\}. \quad (52)$$

The code also supports logical Pauli operators $\bar{X}_\ell, \bar{Y}_\ell, \bar{Z}_\ell$ for $\ell = 1, 2, \dots, k$. They satisfy two requirements. First, within each logical qubit they obey the usual Pauli algebra. For example,

$$\bar{X}_\ell \bar{Z}_\ell = -\bar{Z}_\ell \bar{X}_\ell, \quad \bar{Y}_\ell = i \bar{X}_\ell \bar{Z}_\ell. \quad (53)$$

Operators on different logical qubits commute. Second, every logical Pauli commutes with every stabilizer generator:

$$[P_i, \bar{X}_\ell] = [P_i, \bar{Y}_\ell] = [P_i, \bar{Z}_\ell] = 0 \quad \text{for all } i, \ell. \quad (54)$$

These logical operators act nontrivially inside \mathcal{C} . They generate the encoded qubits. Two physical Pauli operators that differ by an element of \mathcal{S} act in the same way on \mathcal{C} . So they represent the same logical operation.

Because all generators commute and satisfy $P_i^2 = I$, the projector onto the code space has a simple form. Let $|\mathcal{S}|$ be the size of the stabilizer group. Then

$$P_{\mathcal{C}} = \frac{1}{|\mathcal{S}|} \sum_{S \in \mathcal{S}} S. \quad (55)$$

This is equivalent to the product form

$$P_{\mathcal{C}} = \prod_{i=1}^m \frac{I + P_i}{2}. \quad (56)$$

Each factor $\frac{I + P_i}{2}$ projects onto the +1 eigenspace of P_i . Since the factors commute, the product projects onto the joint eigenspace.

A valid encoded state must be supported only on the code space. Algebraically, this means

$$\rho = P_{\mathcal{C}} \rho P_{\mathcal{C}}. \quad (57)$$

Given any physical state ρ_{phys} on the full Hilbert space, we can project it into the code by

$$\rho_L := \frac{P_{\mathcal{C}} \rho_{\text{phys}} P_{\mathcal{C}}}{\text{Tr}(P_{\mathcal{C}} \rho_{\text{phys}})}. \quad (58)$$

In what follows, when we say logical state ρ_L , we always mean a state that satisfies $\rho_L = P_{\mathcal{C}} \rho_L P_{\mathcal{C}}$.

Now assume that the code encodes one logical qubit. Let

$$V : \mathbb{C}^2 \rightarrow \mathcal{H}, \quad V^\dagger V = I, \quad V V^\dagger = P_{\mathcal{C}}, \quad (59)$$

be an encoding isometry.

We choose Pauli-string representatives

$$\bar{X}, \bar{Y}, \bar{Z} \in \mathcal{N}(\mathcal{S}) \setminus \mathcal{S} \quad (60)$$

for the encoded Pauli operators. These representatives are defined only up to multiplication by stabilizers. On the code space, they satisfy

$$P_C \bar{X} P_C = V \sigma_x V^\dagger, \quad P_C \bar{Y} P_C = V \sigma_y V^\dagger, \quad P_C \bar{Z} P_C = V \sigma_z V^\dagger. \quad (61)$$

A general logical state on the abstract qubit can be written as

$$\rho_{\log} = \frac{1}{2} (I + \alpha_x \sigma_x + \alpha_y \sigma_y + \alpha_z \sigma_z), \quad \|\vec{\alpha}\| \leq 1. \quad (62)$$

The corresponding physical encoded state is

$$\rho_L = V \rho_{\log} V^\dagger = P_C \frac{I + \alpha_x \bar{X} + \alpha_y \bar{Y} + \alpha_z \bar{Z}}{2} P_C. \quad (63)$$

Here $\vec{\alpha} = (\alpha_x, \alpha_y, \alpha_z)$ is the Bloch vector of the encoded qubit. The condition $\|\vec{\alpha}\| \leq 1$ ensures positivity. The projectors ensure that ρ_L is supported only on \mathcal{C} .

The action of a physical Pauli operator $Q \in \mathcal{P}_n$ is determined by how it (anti)commutes with the stabilizers. The set of all Paulis that commute with every stabilizer is the normalizer:

$$\mathcal{N}(\mathcal{S}) = \{Q \in \mathcal{P}_n \mid [Q, P_i] = 0 \text{ for all } i\}. \quad (64)$$

Any element of $\mathcal{N}(\mathcal{S})$ preserves the code space. Two operators that differ by a stabilizer element act identically on \mathcal{C} . Therefore, distinct logical operations are labeled by the quotient group

$$\mathcal{N}(\mathcal{S})/\mathcal{S}. \quad (65)$$

When we measure a Pauli operator Q on a code state, there are three basic cases.

- (1) If $Q \in \mathcal{S}$, the outcome is deterministically +1 and the state does not change.
- (2) If $Q \in \mathcal{N}(\mathcal{S}) \setminus \mathcal{S}$, then Q acts as a nontrivial logical Pauli. Measuring it performs a logical measurement on the encoded qubit.
- (3) If $Q \notin \mathcal{N}(\mathcal{S})$, then Q anticommutes with at least one stabilizer generator. As an error operator, it creates a nonzero syndrome and is not a logical Pauli. As a measurement operator, however, it can be used to update the stabilizer group, provided that we replace one anticommuting stabilizer by the measured operator and track the measurement outcome.

Assume that Q anticommutes with at least one stabilizer generator. By relabeling the generators, we may assume

$$\{Q, P_1\} = 0. \quad (66)$$

We now change the generating set *within the same stabilizer group*. This is a GF(2) basis change that uses only products of stabilizers.

For $j \geq 2$, define

$$\tilde{P}_1 := P_1, \quad \tilde{P}_j := \begin{cases} P_j, & [Q, P_j] = 0, \\ P_j P_1, & \{Q, P_j\} = 0. \end{cases} \quad (67)$$

Each \tilde{P}_j lies in \mathcal{S} , since it is a product of the original generators. The map is invertible over GF(2). If $[Q, P_j] = 0$, then $P_j = \tilde{P}_j$. If $\{Q, P_j\} = 0$, then $P_j = \tilde{P}_j \tilde{P}_1$. Therefore, the set $\{\tilde{P}_1, \dots, \tilde{P}_m\}$ generates the same group \mathcal{S} .

With this choice, Q anticommutes with only one generator. We have

$$\{Q, \tilde{P}_1\} = 0, \quad [Q, \tilde{P}_j] = 0 \quad (j \geq 2). \quad (68)$$

The second relation follows because, when $\{Q, P_j\} = 0$, we also have $\{Q, P_1\} = 0$. Thus Q commutes with the product $P_j P_1$.

We can also adjust logical Pauli representatives without changing their logical action. Let $\bar{L} \in \mathcal{N}(\mathcal{S})$ be a chosen physical representative of a logical Pauli operator. Since $\tilde{P}_1 \in \mathcal{S}$, the two operators \bar{L} and $\bar{L}\tilde{P}_1$ act in the same way on the code space. Indeed, for any code state $|\psi\rangle \in \mathcal{C}$,

$$\bar{L}\tilde{P}_1|\psi\rangle = \bar{L}|\psi\rangle. \quad (69)$$

Thus multiplying a logical representative by \tilde{P}_1 changes only the physical representative, not the encoded logical operation.

If \bar{L} anticommutes with Q , we replace it by $\bar{L}\tilde{P}_1$. Since $\{Q, \tilde{P}_1\} = 0$, this flips the commutation sign. As a result, the new representative commutes with Q . After this step, we may assume that all chosen logical Pauli operators commute with Q .

With these choices, measuring Q changes only one stabilizer eigenvalue. It does not disturb the logical information. The measurement projectors are

$$\Pi_{\pm} = \frac{I \pm Q}{2}, \quad (70)$$

and the conditional post-measurement states are

$$\rho_{\pm} = \frac{\Pi_{\pm}\rho\Pi_{\pm}}{p_{\pm}}, \quad p_{\pm} = \text{Tr}(\rho\Pi_{\pm}). \quad (71)$$

For a code state ρ stabilized by \tilde{P}_1 , the anticommutation $\{Q, \tilde{P}_1\} = 0$ implies

$$\text{Tr}(\rho Q) = 0, \quad (72)$$

and therefore

$$p_+ = p_- = \frac{1}{2}. \quad (73)$$

Because Q commutes with \tilde{P}_j for $j \geq 2$ and also commutes with all logical operators (after the redefinitions above), the logical Bloch vector \vec{a} is unchanged by the measurement. The only change is that the old stabilizer generator \tilde{P}_1 is replaced by the signed measured operator $\pm Q$.

Thus the measurement replaces the old generator \tilde{P}_1 by the signed measured operator $\pm Q$. The post-measurement stabilizer group is

$$\mathcal{S}'_{\pm} = \langle \pm Q, \tilde{P}_2, \dots, \tilde{P}_m \rangle. \quad (74)$$

The sign is the measurement outcome and is recorded in the Pauli frame. Since the chosen logical representatives commute with Q , the encoded logical state is preserved up to this known frame update.

Equivalently, the projector onto the post-measurement stabilized subspace can be written as

$$P_C^{(\pm)} = \frac{I \pm Q}{2} \prod_{j=2}^m \frac{I + \tilde{P}_j}{2}. \quad (75)$$

So the stabilizer configuration is updated, but the encoded logical qubit is not. This is the key point we will use later: local Pauli measurements can move or reshape defects by changing stabilizers, while the logical information remains invariant.

We now explain how the measurement update above leads to a sequential sensing protocol. The key point is the following. A local Pauli measurement can change the stabilizers. It can move a defect by one cell. At the same time, it does not change the encoded logical state.

Later we will specialize to a planar surface-code patch. We will use a planar graph $G = (V, E, F)$. A Z -type string operator is specified by a 1-chain

$$c \in C_1(G; \mathbb{F}_2) \cong \mathbb{F}_2^E, \quad (76)$$

and we write the corresponding Pauli as $Z(c)$. For a fixed defect configuration, we call c *legal* if it has no endpoints on active vertices. Legal Z -chains preserve the code space. They implement either stabilizers or logical Z operators. We denote the logical Z operator by \bar{Z} .

The measurement result above implies a transport rule for the logical qubit. Consider a sequence of code configurations indexed by $r = 1, 2, \dots, L$. Let $\mathcal{S}^{(r)}$ be the stabilizer group at step r . Let $P_C^{(r)}$ be the corresponding code projector. Between step r and $r+1$ we measure a local Pauli Q_r . This measurement updates the stabilizers and moves the defect by one cell. The logical information is preserved. Any required update is classical.

We use this to load Z -signals in time. At each step r we choose a legal chain c_r for the current logical Z configuration. We choose the sequence so that all $Z(c_r)$ act as the same logical operator on the code space. Equivalently, they represent the same physical implementation of \bar{Z} , up to stabilizers.

We now describe the sequential schedule in the same normalization as the main text. The normalized target is

$$q = \sum_{\alpha} s_{\alpha} \lambda_{\alpha}, \quad |s_{\alpha}| \leq 1, \quad \max_{\alpha} |s_{\alpha}| = 1. \quad (77)$$

At dwell step r , the current defect configuration is chosen so that one intended signal chain c_r has a nonzero logical projection. After the known Pauli-frame identification between consecutive code spaces, this chain represents the same logical operator \bar{Z} . Thus, in the effective code-space description,

$$P_C^{(r)} Z(c_r) P_C^{(r)} = P_C^{(r)} \bar{Z} P_C^{(r)}. \quad (78)$$

If this step senses the coupling λ_{α_r} for a dwell time τ_r , then its logical contribution is

$$H_{\text{eff}}^{(r)} = \frac{1}{2} \sigma_r \lambda_{\alpha_r} \bar{Z}, \quad \sigma_r \in \{\pm 1\}, \quad (79)$$

where σ_r records whether an echo operation reverses the sign.

In summary, local measurements let us move defects while keeping the encoded qubit intact. This makes it possible to sense many local couplings with a single logical qubit. The target weights are programmed in time.

SUP2 CHAIN AND COCHAIN NOTATION AND THE GLOBAL ODD-WITNESS CRITERION

We first fix the physical cell complex used in this section. Let

$$G_{\text{phys}} = (V, E, F_{\text{int}}) \quad (80)$$

be the physical planar patch. Its underlying space is homeomorphic to a closed disk. The edge set E labels data qubits, and F_{int} labels the physical plaquettes.

For homological analysis, we add the unbounded exterior region as one extra face f_{∞} and set

$$G = (V, E, F), \quad F = F_{\text{int}} \cup \{f_{\infty}\}. \quad (81)$$

This operation does not identify opposite boundary points. It does not turn the planar patch into a torus. It only turns the planar cellulation into a cellulation of a sphere. Hence

$$H_1(G; \mathbb{F}_2) = 0. \quad (82)$$

Unless stated otherwise, all chain and cochain groups below are those of this extended complex G .

All chains and cochains are over $\mathbb{F}_2 = \{0, 1\}$. Addition is XOR, denoted by \oplus .

We view G as a chain complex over \mathbb{F}_2 . The chain spaces are

$$C_0(G; \mathbb{F}_2) \cong \mathbb{F}_2^V, \quad C_1(G; \mathbb{F}_2) \cong \mathbb{F}_2^E, \quad C_2(G; \mathbb{F}_2) \cong \mathbb{F}_2^F. \quad (83)$$

Thus a chain is a 0/1 indicator vector on vertices, edges, or faces. The boundary maps are

$$\partial_1 : C_1 \rightarrow C_0, \quad \partial_2 : C_2 \rightarrow C_1. \quad (84)$$

In matrix form, we write the edge–vertex incidence matrix as

$$D : \mathbb{F}_2^E \rightarrow \mathbb{F}_2^V, \quad Dc = \partial_1 c, \quad (85)$$

and the face–edge incidence matrix as

$$B : \mathbb{F}_2^F \rightarrow \mathbb{F}_2^E, \quad Bs = \partial_2 s. \quad (86)$$

Thus Dc gives the endpoint parity vector of an edge set c , and Bs gives the XOR sum of selected plaquette boundaries.

Cochains are linear functionals on chains. Over \mathbb{F}_2 , we identify them with the same vector spaces:

$$C^0(G; \mathbb{F}_2) \cong \mathbb{F}_2^V, \quad C^1(G; \mathbb{F}_2) \cong \mathbb{F}_2^E, \quad C^2(G; \mathbb{F}_2) \cong \mathbb{F}_2^F. \quad (87)$$

The coboundary operators are the transposes of the boundary matrices:

$$\delta^0 = D^\top : C^0 \rightarrow C^1, \quad \delta^1 = B^\top : C^1 \rightarrow C^2. \quad (88)$$

In this supplement, we use the symbol w more broadly than in the main text. Here w may denote an arbitrary dual 1-cochain in $C^1(G; \mathbb{F}_2)$, not necessarily a simple closed dual loop. This broader use does not change the main argument. Indeed, the algebraic criterion first gives a closed dual 1-cochain, and the later simple-witness step shows that one may choose a simple representative when the main-text construction requires one.

A 1-cochain $w \in C^1(G; \mathbb{F}_2)$ is a 1-cocycle iff

$$B^\top w = 0. \quad (89)$$

Since the outer face is included in B , this condition also checks the outer dual vertex. Geometrically, the dual support of w has even degree at every dual vertex. Thus it has no boundary as a mod-2 dual 1-chain. In general, this support need not be a single simple loop. It is an even dual subgraph, and it may be a union of closed dual cycles.

On a simply connected patch, every 1-cocycle is a coboundary. This gives a binary potential on vertices, or equivalently a global 0/1 coloring. This is the basic algebraic tool used below.

Proposition S2.1 (Cocycle–potential correspondence). Let G be the extended complex obtained from the physical planar patch by adding the outer face. Since G is topologically a sphere,

$$H_1(G; \mathbb{F}_2) = 0. \quad (90)$$

Let $w \in C^1(G; \mathbb{F}_2)$ satisfy $B^\top w = 0$. Then:

(i) There exists a 0-cochain $t \in C^0(G; \mathbb{F}_2) \cong \mathbb{F}_2^V$ such that

$$w = D^\top t. \quad (91)$$

Equivalently, for every edge $e = (u, v)$,

$$w_e = t(u) \oplus t(v). \quad (92)$$

(ii) The potential t is unique up to a global flip. If t' also satisfies $w = D^\top t'$, then there exists a constant $c \in \{0, 1\}$ such that

$$t'(v) = t(v) \oplus c \quad \text{for all } v \in V. \quad (93)$$

So a closed dual 1-cocycle is exactly the coboundary of a binary vertex coloring. Equivalently, it is the set of edges across which the coloring changes. The coloring is unique up to flipping all colors.

Proof. We construct t by a path-sum rule and then prove it is well defined.

First, we show that w has zero pairing with any closed 1-chain. Let $C \in C_1(G; \mathbb{F}_2)$ satisfy $\partial_1 C = 0$. Since $H_1(G; \mathbb{F}_2) = 0$, there exists $S \in C_2(G; \mathbb{F}_2)$ such that

$$C = \partial_2 S = BS. \quad (94)$$

Using the standard pairing

$$\langle w, C \rangle := \sum_{e \in E} w_e C_e \in \mathbb{F}_2, \quad (95)$$

we compute

$$\langle w, C \rangle = \langle w, BS \rangle = \langle B^\top w, S \rangle. \quad (96)$$

Because $B^\top w = 0$, we get

$$\langle w, C \rangle = 0. \quad (97)$$

In words, the XOR sum of w_e along any closed edge set is 0.

Next we define t . Choose a reference vertex $v_0 \in V$ and set

$$t(v_0) := 0. \quad (98)$$

For any vertex $v \in V$, pick a path π from v_0 to v ,

$$\pi : v_0 \rightarrow v_1 \rightarrow \cdots \rightarrow v_k = v, \quad (99)$$

with edges $e_i = (v_{i-1}, v_i)$. Define

$$t(v) := \bigoplus_{i=1}^k w_{e_i}. \quad (100)$$

Thus $t(v)$ is the parity of the edges in the chosen path on which $w_e = 1$.

We now show that this does not depend on the chosen path. Let π_1 and π_2 be two paths from v_0 to v . Regard them as 1-chains over \mathbb{F}_2 . Their XOR sum

$$C := \pi_1 \oplus \pi_2 \quad (101)$$

is a closed 1-chain, because endpoints cancel in \mathbb{F}_2 . By the closed-chain result above,

$$\langle w, C \rangle = 0. \quad (102)$$

This is exactly

$$\bigoplus_{e \in \pi_1} w_e = \bigoplus_{e \in \pi_2} w_e. \quad (103)$$

Therefore $t(v)$ is path independent. So t is a well-defined 0-cochain on V .

We now prove $w = D^\top t$. Take any edge $e = (u, v)$. Choose a path π_u from v_0 to u , and extend it by e to get a path π_v from v_0 to v . By definition,

$$t(v) = t(u) \oplus w_e. \quad (104)$$

Rearranging gives

$$w_e = t(u) \oplus t(v). \quad (105)$$

Since this holds for every edge, we obtain $w = D^\top t$. This proves (i).

Finally we prove (ii). Suppose t and t' both satisfy $w = D^\top t = D^\top t'$. Define $s := t \oplus t'$. Then

$$D^\top s = D^\top t \oplus D^\top t' = w \oplus w = 0. \quad (106)$$

So for every edge (u, v) ,

$$s(u) \oplus s(v) = 0. \quad (107)$$

Hence $s(u) = s(v)$ on every adjacent pair. Since the graph is connected, s is a constant $c \in \{0, 1\}$ on all vertices. Equivalently,

$$t'(v) = t(v) \oplus c \quad \text{for all } v \in V. \quad (108)$$

This is exactly a global flip. The proposition is proved. \square

We now apply the cocycle–potential correspondence to the prescribed signal chains. This step concerns the global parity structure. It does not yet construct rough holes.

Let \mathcal{I} be the set of signal labels. For each $\alpha \in \mathcal{I}$, let $c_\alpha \in C_1(G; \mathbb{F}_2)$ be a simple primal path with endpoints u_α and v_α . Thus

$$Dc_\alpha = u_\alpha \oplus v_\alpha. \quad (109)$$

Here we identify a vertex with the corresponding basis vector in $C_0(G; \mathbb{F}_2)$.

Define the endpoint graph Γ_{end} as follows. Its vertex set is the set of all endpoints that appear among the chains. For each signal chain c_α , we add one abstract edge η_α between u_α and v_α . This graph is an abstract multigraph. The edge η_α records only the two endpoints of c_α . It does not record the full geometric shape of c_α .

We also use the following terminology. A *simple odd witness* is a simple closed dual loop w_s such that

$$\langle w_s, c_\alpha \rangle = 1 \quad \text{for all } \alpha \in \mathcal{I}. \quad (110)$$

Geometrically, w_s is a simple closed curve in dual position. It is transverse to primal edges and avoids primal vertices. Algebraically, it is represented by the 1-cochain that records which primal edges it crosses. Thus $B^\top w_s = 0$.

Proposition S2.2 (Global odd-parity and simple-witness criterion). The following four statements are equivalent.

(i) There exists a 1-cochain $w_{\text{alg}} \in C^1(G; \mathbb{F}_2)$ such that

$$B^\top w_{\text{alg}} = 0, \quad \langle w_{\text{alg}}, c_\alpha \rangle = 1 \quad \text{for all } \alpha \in \mathcal{I}. \quad (111)$$

(ii) The endpoint graph Γ_{end} is bipartite.

(iii) There is no subset $\mathcal{A} \subseteq \mathcal{I}$ such that $|\mathcal{A}|$ is odd and

$$D \left(\bigoplus_{\alpha \in \mathcal{A}} c_\alpha \right) = 0. \quad (112)$$

(iv) There exists a simple odd witness w_s , namely a simple closed dual loop, such that

$$\langle w_s, c_\alpha \rangle = 1 \quad \text{for all } \alpha \in \mathcal{I}. \quad (113)$$

Proof. We first prove the equivalence of (i), (ii), and (iii). Then we prove that (ii) is also equivalent to the simple-witness statement (iv).

First, we prove that (i) implies (ii). Assume that w_{alg} exists. Since $B^\top w_{\text{alg}} = 0$, Proposition S2.1 gives a 0-cochain $t \in C^0(G; \mathbb{F}_2)$ such that

$$w_{\text{alg}} = D^\top t. \quad (114)$$

For each signal chain c_α , we have

$$1 = \langle w_{\text{alg}}, c_\alpha \rangle = \langle D^\top t, c_\alpha \rangle = \langle t, Dc_\alpha \rangle = t(u_\alpha) \oplus t(v_\alpha). \quad (115)$$

Thus the two endpoints of every endpoint edge η_α have opposite colors under t . Hence Γ_{end} is bipartite.

Next, we prove that (ii) implies (i). Assume that Γ_{end} is bipartite. Choose a binary coloring of its vertices, still denoted by t , such that

$$t(u_\alpha) \oplus t(v_\alpha) = 1 \quad \text{for all } \alpha \in \mathcal{I}. \quad (116)$$

Extend t arbitrarily to all vertices of G . Define

$$w_{\text{alg}} := D^\top t. \quad (117)$$

Then

$$B^\top w_{\text{alg}} = B^\top D^\top t = (DB)^\top t = 0, \quad (118)$$

because $DB = 0$. Also, for each α ,

$$\langle w_{\text{alg}}, c_\alpha \rangle = \langle D^\top t, c_\alpha \rangle = \langle t, Dc_\alpha \rangle = t(u_\alpha) \oplus t(v_\alpha) = 1. \quad (119)$$

Thus the algebraic closed dual parity test exists. This proves the equivalence of (i) and (ii).

It remains to prove the equivalence between (ii) and (iii). For clarity, we introduce the boundary map of the endpoint graph. Let

$$\partial_{\text{end}} : C_1(\Gamma_{\text{end}}; \mathbb{F}_2) \rightarrow C_0(\Gamma_{\text{end}}; \mathbb{F}_2) \quad (120)$$

be the \mathbb{F}_2 -linear map defined on each endpoint edge by

$$\partial_{\text{end}} \eta_\alpha = u_\alpha \oplus v_\alpha. \quad (121)$$

By definition of the endpoints of c_α , we have

$$\partial_{\text{end}}\eta_\alpha = Dc_\alpha. \quad (122)$$

Therefore, for every subset $\mathcal{A} \subseteq \mathcal{I}$,

$$\partial_{\text{end}}\left(\bigoplus_{\alpha \in \mathcal{A}} \eta_\alpha\right) = D\left(\bigoplus_{\alpha \in \mathcal{A}} c_\alpha\right). \quad (123)$$

Thus

$$D\left(\bigoplus_{\alpha \in \mathcal{A}} c_\alpha\right) = 0 \quad (124)$$

if and only if the selected endpoint edges $\{\eta_\alpha : \alpha \in \mathcal{A}\}$ form a closed 1-chain in Γ_{end} over \mathbb{F}_2 .

We now prove that (ii) implies (iii). Assume that Γ_{end} is bipartite. Let its two vertex classes be V_0 and V_1 . Then every endpoint edge has one endpoint in V_0 and one endpoint in V_1 .

Suppose that $\mathcal{A} \subseteq \mathcal{I}$ satisfies

$$D\left(\bigoplus_{\alpha \in \mathcal{A}} c_\alpha\right) = 0. \quad (125)$$

By Eq. (123), this is equivalent to

$$\partial_{\text{end}}\left(\bigoplus_{\alpha \in \mathcal{A}} \eta_\alpha\right) = 0. \quad (126)$$

For a vertex $x \in V_{\text{end}}$, let $\deg_{\mathcal{A}}(x)$ be the number of selected endpoint edges incident to x . The equation above says that every vertex has even selected degree:

$$\deg_{\mathcal{A}}(x) \equiv 0 \pmod{2} \quad \text{for every } x \in V_{\text{end}}. \quad (127)$$

Now count the selected endpoint edges from the V_0 side. Since every selected endpoint edge has exactly one endpoint in V_0 , we have the integer equality

$$|\mathcal{A}| = \sum_{x \in V_0} \deg_{\mathcal{A}}(x). \quad (128)$$

Each term on the right-hand side is even. Therefore $|\mathcal{A}|$ is even. Hence no odd-cardinality subset \mathcal{A} can satisfy Eq. (112). This proves (iii).

Next, we prove that (iii) implies (ii). We prove the contrapositive. Assume that Γ_{end} is not bipartite. Then Γ_{end} contains an odd cycle. Let the endpoint edges on this odd cycle be

$$\eta_{\alpha_1}, \eta_{\alpha_2}, \dots, \eta_{\alpha_{2k+1}}. \quad (129)$$

Set

$$\mathcal{A} = \{\alpha_1, \alpha_2, \dots, \alpha_{2k+1}\}. \quad (130)$$

Then $|\mathcal{A}| = 2k + 1$, so \mathcal{A} has odd cardinality.

The selected endpoint edges form a cycle. Hence every vertex on this cycle has selected degree 2, and every other vertex has selected degree 0. Therefore

$$\partial_{\text{end}}\left(\bigoplus_{\alpha \in \mathcal{A}} \eta_\alpha\right) = 0. \quad (131)$$

Using Eq. (123), we obtain

$$D\left(\bigoplus_{\alpha \in \mathcal{A}} c_\alpha\right) = 0. \quad (132)$$

Thus there exists an odd-cardinality subset \mathcal{A} whose physical boundary cancels. This violates (iii). Therefore, if (iii) holds, Γ_{end} must be bipartite.

This proves the equivalence of (ii) and (iii).

It remains to relate the bipartition to a simple witness. We first prove that (ii) implies (iv). Assume that Γ_{end} is bipartite. Choose a bipartition of its endpoint vertices,

$$U_0 \sqcup U_1. \quad (133)$$

Thus each signal chain has one endpoint in U_0 and one endpoint in U_1 . Write

$$Dc_\alpha = u_\alpha^{(0)} \oplus u_\alpha^{(1)}, \quad u_\alpha^{(0)} \in U_0, \quad u_\alpha^{(1)} \in U_1. \quad (134)$$

We work on the sphere obtained by adding the outer face. Choose an embedded tree T_0 on the sphere such that

$$U_0 \subset T_0, \quad T_0 \cap U_1 = \emptyset. \quad (135)$$

This is possible because U_0 and U_1 are finite sets of points on the sphere. We connect the points in U_0 by embedded arcs, and choose the arcs to avoid the finite set U_1 . If the union has extra cycles, we take a spanning tree of that union.

Let $N(T_0)$ be a small closed regular neighborhood of T_0 , chosen so that

$$U_0 \subset \text{int } N(T_0), \quad U_1 \cap N(T_0) = \emptyset. \quad (136)$$

Since T_0 is a tree, $N(T_0)$ is a disk. Hence its boundary $\partial N(T_0)$ is a simple closed curve. We choose the separating curve γ so that it crosses the primal cellulation cleanly: it may cross primal edges, but only through their interior points. It does not pass through primal vertices and does not overlap with any primal edge. Let $w_s \in C^1(G; \mathbb{F}_2)$ record, for each primal edge, whether γ crosses that edge an odd number of times.

The curve w_s separates the sphere into two sides. One side contains U_0 , and the other side contains U_1 . Fix any signal path c_α . It starts at $u_\alpha^{(0)} \in U_0$ and ends at $u_\alpha^{(1)} \in U_1$. Thus its endpoints lie on different sides of w_s . Each time c_α crosses w_s , it changes side. Therefore the number of crossings is odd. Hence

$$\langle w_s, c_\alpha \rangle = 1 \quad \text{for all } \alpha \in \mathcal{I}. \quad (137)$$

Thus a simple odd witness exists. This proves (iv).

Finally, (iv) implies (i). Indeed, a simple closed dual loop has no endpoints, so its associated 1-cochain satisfies

$$B^\top w_s = 0. \quad (138)$$

Together with Eq. (113), this is exactly statement (i), with $w_{\text{alg}} = w_s$.

All four statements are equivalent. \square

Remark. The proposition separates two ideas. The algebraic object in statement (i) is a closed dual parity test. Its support may be a union of closed dual cycles. It need not be one simple loop.

The planar geometry gives more. Statement (iv) says that, once the endpoint graph is bipartite, we can construct a simple odd witness. We do not obtain this simple loop by choosing one connected component of the algebraic w_{alg} . Instead, we use the endpoint bipartition. We connect one endpoint class by a tree, thicken the tree to a disk, and take the boundary of that disk. This boundary is a simple closed dual loop. Since every signal path has endpoints on opposite sides, every signal path crosses this loop oddly.

The obstruction in the global criterion is not the existence of a closed 1-cycle in the union of the signal chains. The obstruction is an odd closed dependency among the signal chains. Thus an even closed dependency is allowed. For example, four chains may satisfy

$$D(c_1 \oplus c_2 \oplus c_3 \oplus c_4) = 0, \quad (139)$$

and still admit a simple odd witness, because

$$1 \oplus 1 \oplus 1 \oplus 1 = 0. \quad (140)$$

In contrast, three chains satisfying

$$D(c_1 \oplus c_2 \oplus c_3) = 0 \quad (141)$$

cannot all pair oddly with a closed witness, because

$$1 \oplus 1 \oplus 1 = 1. \quad (142)$$

This distinction explains the role of Fig. 4 in the main text. That figure may satisfy the global odd-witness criterion even though the signal chains form a closed cycle. Its possible failure is local. It belongs to the clean rough-hole realization step, not to the global witness criterion.

Corollary S2.3 (Useful sufficient cases). The following two sufficient conditions imply that a simple odd witness exists.

- (i) If the endpoint graph Γ_{end} is a forest, then a simple odd witness exists.
- (ii) Assume the signal chains are edge-disjoint. If the physical union graph

$$\Gamma_{\text{sig}} := \bigcup_{\alpha \in \mathcal{I}} c_{\alpha} \quad (143)$$

has no cycle, then a simple odd witness exists.

Proof. For (i), a forest is bipartite. Hence Proposition S2.2 gives a simple odd witness.

For (ii), it is enough to show that Γ_{end} is a forest. Suppose not. Then Γ_{end} contains a cycle with endpoint edges

$$\eta_{\alpha_1}, \eta_{\alpha_2}, \dots, \eta_{\alpha_m}. \quad (144)$$

Let

$$\mathcal{A} = \{\alpha_1, \alpha_2, \dots, \alpha_m\}. \quad (145)$$

Since these endpoint edges form a cycle,

$$\partial_{\text{end}} \left(\bigoplus_{\alpha \in \mathcal{A}} \eta_{\alpha} \right) = 0. \quad (146)$$

Using the relation

$$\partial_{\text{end}} \eta_{\alpha} = D c_{\alpha}, \quad (147)$$

we get

$$D \left(\bigoplus_{\alpha \in \mathcal{A}} c_{\alpha} \right) = 0. \quad (148)$$

Define

$$z_{\text{sig}} := \bigoplus_{\alpha \in \mathcal{A}} c_{\alpha}. \quad (149)$$

Then $D z_{\text{sig}} = 0$. Also $z_{\text{sig}} \neq 0$, because the selected signal chains are edge-disjoint and therefore their edges cannot cancel.

Thus z_{sig} is a nonzero closed 1-chain in the finite graph Γ_{sig} . The support of any nonzero closed 1-chain in a finite graph contains an ordinary graph cycle. Hence Γ_{sig} contains a cycle. This contradicts the assumption that Γ_{sig} has no cycle.

Therefore Γ_{end} is a forest. By (i), a simple odd witness exists. \square

SUP3 CONSTRUCTING ROUGH HOLES FROM SIMPLE WITNESSES

We use the notation of SUP2. Thus G is the extended planar complex obtained from the physical patch by adding the outer face. We view G as a cellulation of the sphere. All chains and cochains are over \mathbb{F}_2 . The edge–vertex incidence matrix is D , and the face–edge incidence matrix is B .

Let

$$\{c_{\alpha} : \alpha \in \mathcal{I}\} \subset C_1(G; \mathbb{F}_2) \quad (150)$$

be the prescribed signal chains. Each c_α is the 1-chain supported on a simple primal path. We assume the disjoint-support regime.

The purpose of this section is not to prove the global odd-witness criterion again. That criterion was proved in SUP2. In particular, Proposition S2.2 shows that the compatible case is equivalent to the existence of a simple odd witness. Here we explain how such simple witnesses guide the construction of two actual rough holes.

The construction has two stages. First, a simple odd witness on the original patch gives a witness-guided region Ω_0 . We then choose a clean actual rough hole $R_0 \subseteq \Omega_0$. Second, after R_0 is created, we collapse R_0 to one rough vertex. On the quotient complex, Proposition S2.2 again gives a simple odd witness. This second witness gives a witness-guided region Ω_1 . We then choose a clean actual rough hole $R_1 \subseteq \Omega_1$.

By Proposition S2.2, the compatible case gives a simple odd witness $w^{(1)}$. Thus $w^{(1)}$ is a simple closed dual loop and

$$\langle w^{(1)}, c_\alpha \rangle = 1 \quad \text{for all } \alpha \in \mathcal{I}. \quad (151)$$

Equivalently, $w^{(1)}$ separates the sphere into two connected sides. Since c_α crosses $w^{(1)}$ oddly, the two endpoints of c_α lie on opposite sides of $w^{(1)}$. We choose one side and call it Ω_0 . More precisely, Ω_0 denotes the witness-guided check region on this side. We use the same symbol for a check-vertex region and for its disk-like carrier subcomplex. Let U_0 be the set of endpoints of the signal chains lying in Ω_0 :

$$U_0 := \{u_\alpha^{(0)} : \alpha \in \mathcal{I}\}. \quad (152)$$

For each α , the other endpoint of c_α is denoted by $u_\alpha^{(1)}$. Thus

$$Dc_\alpha = u_\alpha^{(0)} \oplus u_\alpha^{(1)}, \quad u_\alpha^{(0)} \in \Omega_0, \quad u_\alpha^{(1)} \notin \Omega_0. \quad (153)$$

The region Ω_0 is only a guide. It is not itself the rough hole. No star check is turned off only because it lies in Ω_0 . The actual first rough hole is a connected disk-like check region

$$R_0 \subseteq \Omega_0. \quad (154)$$

It must contain the endpoint set U_0 :

$$U_0 \subseteq R_0. \quad (155)$$

It must also satisfy the clean condition. The non-terminal part of a prescribed signal chain c_α is the part away from its endpoint contact with the rough boundary. Equivalently, a non-terminal vertex of c_α is a star-check vertex where the path passes through rather than ends. In the simple-path case considered here, this means that two edges of c_α meet at that vertex. If v is a non-terminal vertex of any prescribed signal chain c_α , then the star check at v is not included in R_0 . Equivalently, that star check is kept active.

This is a local geometric condition. It is not part of the global odd-witness criterion. If no such clean connected R_0 can be chosen inside Ω_0 , then the simple odd witness exists, but this local rough-hole implementation fails.

When R_0 is chosen, we turn off exactly the selected X -type star checks in R_0 . This creates the first rough boundary. After this operation, each signal chain c_α has one endpoint on the rough boundary created by R_0 , while its interior remains in the active code region. In this sense, each c_α terminates on the first rough boundary.

For the quotient notation, we regard R_0 as a small contractible disk-like subcomplex carried by the selected check vertices. We still denote this subcomplex by R_0 . Define

$$\hat{G} := G/R_0 \quad (156)$$

to be the quotient complex obtained by collapsing R_0 to one vertex. We denote the collapsed vertex by \hat{r}_0 . Let

$$\pi_0 : G \rightarrow \hat{G} \quad (157)$$

be the quotient map.

Because R_0 is contractible and disk-like, collapsing R_0 does not create a handle. The quotient \hat{G} is again a planar complex on the sphere. In particular,

$$H_1(\hat{G}; \mathbb{F}_2) = 0. \quad (158)$$

Let

$$\hat{D} : \mathbb{F}_2^{\hat{E}} \rightarrow \mathbb{F}_2^{\hat{V}}, \quad \hat{B} : \mathbb{F}_2^{\hat{F}} \rightarrow \mathbb{F}_2^{\hat{E}} \quad (159)$$

be the incidence matrices of \hat{G} .

Each signal chain c_α induces a quotient chain

$$\hat{c}_\alpha \in C_1(\hat{G}; \mathbb{F}_2). \quad (160)$$

The endpoint $u_\alpha^{(0)} \in R_0$ becomes \hat{r}_0 . The other endpoint $u_\alpha^{(1)}$ remains outside R_0 . We write

$$\hat{u}_\alpha := \pi_0(u_\alpha^{(1)}). \quad (161)$$

Thus

$$\hat{D}\hat{c}_\alpha = \hat{r}_0 \oplus \hat{u}_\alpha. \quad (162)$$

Let

$$\hat{U}_1 := \{\hat{u}_\alpha : \alpha \in \mathcal{I}\} \subseteq \hat{V}. \quad (163)$$

We now construct the second witness on \hat{G} . The quotient chains \hat{c}_α all have one endpoint at \hat{r}_0 and the other endpoint in \hat{U}_1 . Therefore the endpoint multigraph of the quotient chains is bipartite, with bipartition $\{\hat{r}_0\} \sqcup \hat{U}_1$. Hence Proposition S2.2 applies on the quotient complex \hat{G} .

Thus there exists a simple odd witness $w^{(2)}$ on \hat{G} such that

$$\langle w^{(2)}, \hat{c}_\alpha \rangle = 1 \quad \text{for all } \alpha \in \mathcal{I}. \quad (164)$$

We choose $w^{(2)}$ so that it separates \hat{r}_0 from all vertices in \hat{U}_1 . Let $\hat{\Omega}_1$ be the side of $w^{(2)}$ that contains \hat{U}_1 . Then

$$\hat{U}_1 \subset \hat{\Omega}_1, \quad \hat{r}_0 \notin \hat{\Omega}_1. \quad (165)$$

We pull this region back to the original patch and define

$$\Omega_1 := \{v \in V_{\text{phys}} : \pi_0(v) \in \hat{\Omega}_1\}. \quad (166)$$

Since $\hat{r}_0 \notin \hat{\Omega}_1$, the region Ω_1 is disjoint from R_0 . Also, by construction,

$$U_1 := \{u_\alpha^{(1)} : \alpha \in \mathcal{I}\} \subseteq \Omega_1. \quad (167)$$

Again, Ω_1 is only a witness-guided region. It tells us where the second rough hole should be placed. It is not itself the rough hole.

The actual second rough hole is a connected disk-like check region

$$R_1 \subseteq \Omega_1 \quad (168)$$

such that

$$U_1 \subseteq R_1. \quad (169)$$

It must satisfy the same clean condition as R_0 . If v is a non-terminal vertex of any prescribed signal chain c_α , then the star check at v is not included in R_1 . Equivalently, that star check is kept active. Thus a check site may lie in the witness-guided region Ω_1 , but still not belong to the actual rough hole R_1 .

After R_1 is chosen, we turn off exactly the selected X -type star checks in R_1 . Now every signal chain c_α has one endpoint on the rough boundary created by R_0 and one endpoint on the rough boundary created by R_1 . Its interior remains in the active code region. Thus every c_α has only terminal contacts with the two rough boundaries, while its non-terminal part remains in the active code region.

The logic of this section is as follows. Proposition S2.2 gives a simple odd witness in the compatible case. The first simple witness $w^{(1)}$ gives the witness-guided region Ω_0 . If a clean connected actual rough hole $R_0 \subseteq \Omega_0$ can be chosen, we open it and collapse it to one vertex.

On the quotient complex, every quotient signal chain has one endpoint at \hat{r}_0 and the other endpoint in \hat{U}_1 . Hence the endpoint multigraph is bipartite, with one part $\{\hat{r}_0\}$ and the other part \hat{U}_1 . Proposition S2.2 then gives a second simple odd witness $w^{(2)}$. This witness gives the second witness-guided region $\hat{\Omega}_1$. If a clean connected actual rough hole $R_1 \subseteq \Omega_1$ can be chosen, then all signal chains become legal Z strings from R_0 to R_1 .

The simple-witness part is global and topological. The clean choice of R_0 and R_1 is local. These are separate requirements.

SUP4 RELATIVE HOMOLOGY FOR FIXED CLEAN ROUGH HOLES

We keep the notation from SUP2 and SUP3. All chain groups are over \mathbb{F}_2 . Thus addition means symmetric difference, or XOR.

The goal of this section is not to prove the global odd-witness criterion. That criterion was proved in SUP2. Here we prove the fixed-hole part of the construction.

Namely, once two actual clean rough holes R_0 and R_1 are fixed, every legal Z string from R_0 to R_1 represents the same nonzero relative homology class. Therefore all such Z strings act as the same nontrivial logical operator on the punctured-code space.

Conversely, for fixed clean rough holes, a nontrivial bridge class has a dual parity test. This dual test is the witness that crosses every bridge with odd parity.

Let

$$G = (V, E, F) \tag{170}$$

be the extended planar complex obtained by adding the outer face to the physical patch. This is only an auxiliary step. It does not identify opposite boundary points. It only turns the planar patch into a cellulation of the sphere.

The edge set E labels data qubits. The face–edge incidence map is

$$B : \mathbb{F}_2^F \rightarrow \mathbb{F}_2^E. \tag{171}$$

In the usual chain-complex notation, this map is the cellular boundary map $\partial_2 : C_2(G; \mathbb{F}_2) \rightarrow C_1(G; \mathbb{F}_2)$; here we denote it by B to emphasize its incidence-matrix representation. Its image is the span of plaquette boundaries. Adding the outer face does not change this span, because the outer-face boundary is the mod-2 sum of the physical plaquette boundaries.

A Z -type signal support is a binary 1-chain

$$c \in C_1(G; \mathbb{F}_2) \cong \mathbb{F}_2^E. \tag{172}$$

The corresponding Pauli operator is

$$Z(c) := \prod_{e:c_e=1} Z_e. \tag{173}$$

If two chains differ by a plaquette boundary, then the corresponding operators differ by a product of Z -type plaquette stabilizers:

$$c' = c \oplus Bs \implies Z(c') = Z(c) \prod_{f:s_f=1} Z(\partial f). \tag{174}$$

Hence $Z(c)$ and $Z(c')$ act in the same way on the code space.

Now fix two actual rough holes R_0 and R_1 . These are the regions where selected X -type star checks are turned off. They are not the same objects as the witness-guided regions Ω_0 and Ω_1 . The regions Ω_i only guide the construction. The actual rough holes R_i are chosen after the local clean check.

The clean condition is the following. Only endpoint contacts with the rough boundary are allowed. The non-terminal parts of all prescribed signal chains must remain in the active code region. Equivalently, if a star-check vertex is a non-terminal vertex of some prescribed signal chain c_α , then that star check is kept active and is not included in any actual rough hole. Thus a signal chain may pass through a witness-guided region Ω_i , but only its endpoint is allowed to contact the actual rough hole R_i .

For homological analysis, we collapse each actual rough hole to one marked vertex. We write

$$\widehat{G} := G / (R_0 \cup R_1). \tag{175}$$

The two collapsed vertices are denoted by

$$\hat{r}_0 \quad \text{and} \quad \hat{r}_1. \tag{176}$$

We also set

$$A := \{\hat{r}_0, \hat{r}_1\}. \tag{177}$$

This quotient is only an analysis device. Physically, a signal chain terminates on the rough boundary of R_i . In the quotient complex, all allowed endpoints on that rough boundary are identified with the single marked vertex \hat{r}_i . Thus A is the set of allowed endpoints for legal Z -chains.

Let

$$\pi : G \rightarrow \widehat{G} \quad (178)$$

be the quotient map. A physical Z -chain c induces a quotient chain

$$\hat{c} := \pi_{\#}(c) \in C_1(\widehat{G}; \mathbb{F}_2). \quad (179)$$

Here $\pi_{\#}$ means the induced map on chains. In words, \hat{c} is the same chain after the two rough holes have been collapsed to the two marked vertices.

Let

$$\widehat{D} : C_1(\widehat{G}; \mathbb{F}_2) \rightarrow C_0(\widehat{G}; \mathbb{F}_2) \quad (180)$$

be the edge–vertex incidence map of \widehat{G} . Thus $\widehat{D}\hat{c}$ records the endpoints of \hat{c} , counted modulo 2.

A legal Z -chain is a chain whose endpoints lie only on the rough boundaries. After the quotient, this means

$$\widehat{D}\hat{c} \in C_0(A; \mathbb{F}_2). \quad (181)$$

Equivalently, the boundary of \hat{c} is allowed to be nonzero, but it must lie inside the marked set A . This is exactly the meaning of a relative 1-cycle for the pair

$$(\widehat{G}, A). \quad (182)$$

Thus relative homology is the natural language for legal open Z -strings: ordinary homology only sees closed strings, while relative homology also allows endpoints on the chosen set A .

A bridge is a legal chain with one endpoint on each rough hole. Equivalently, after the quotient it satisfies

$$\widehat{D}\hat{c} = \hat{r}_0 \oplus \hat{r}_1. \quad (183)$$

Thus a bridge is an open Z -string from R_0 to R_1 .

We now compute the relative group $H_1(\widehat{G}, A; \mathbb{F}_2)$. We use the long exact sequence of the pair (\widehat{G}, A) . For clarity, we first recall where the relevant part comes from. For any pair $A \subset X$, the relative chain group is defined by

$$C_k(X, A; \mathbb{F}_2) := C_k(X; \mathbb{F}_2) / C_k(A; \mathbb{F}_2). \quad (184)$$

This gives a short exact sequence of chain complexes,

$$0 \rightarrow C_*(A; \mathbb{F}_2) \rightarrow C_*(X; \mathbb{F}_2) \rightarrow C_*(X, A; \mathbb{F}_2) \rightarrow 0. \quad (185)$$

Taking homology gives the long exact sequence

$$\cdots \rightarrow H_1(A) \rightarrow H_1(X) \rightarrow H_1(X, A) \xrightarrow{\partial_{\text{rel}}} H_0(A) \xrightarrow{i_*} H_0(X) \rightarrow H_0(X, A) \rightarrow 0. \quad (186)$$

We apply this to

$$X = \widehat{G}, \quad A = \{\hat{r}_0, \hat{r}_1\}. \quad (187)$$

The set A consists of two points, so it has no one-dimensional cycles:

$$H_1(A; \mathbb{F}_2) = 0. \quad (188)$$

Also, by construction, each actual rough hole is a connected disk-like check region inside a disk-like patch. Collapsing such regions does not create a handle. Hence

$$H_1(\widehat{G}; \mathbb{F}_2) = 0. \quad (189)$$

Finally, \widehat{G} is connected and A is nonempty. Therefore the map

$$i_* : H_0(A; \mathbb{F}_2) \rightarrow H_0(\widehat{G}; \mathbb{F}_2) \quad (190)$$

is onto, and hence

$$H_0(\widehat{G}, A; \mathbb{F}_2) = 0. \quad (191)$$

Thus the relevant part of the long exact sequence reduces to

$$0 \rightarrow H_1(\widehat{G}, A; \mathbb{F}_2) \xrightarrow{\partial_{\text{rel}}} H_0(A; \mathbb{F}_2) \xrightarrow{i_*} H_0(\widehat{G}; \mathbb{F}_2) \rightarrow 0. \quad (192)$$

We now compute the kernel of i_* . Since A has two connected components,

$$H_0(A; \mathbb{F}_2) = \text{span}_{\mathbb{F}_2}\{[\hat{r}_0], [\hat{r}_1]\}. \quad (193)$$

Here $[\hat{r}_i]$ denotes the connected component of the point \hat{r}_i inside A . Since \widehat{G} is connected, $H_0(\widehat{G}; \mathbb{F}_2)$ has one generator. We denote it by $[\widehat{G}]$.

The inclusion-induced map i_* sends both points of A to this same connected component:

$$i_*([\hat{r}_0]) = [\widehat{G}], \quad i_*([\hat{r}_1]) = [\widehat{G}]. \quad (194)$$

Therefore, for $a, b \in \mathbb{F}_2$,

$$i_*(a[\hat{r}_0] \oplus b[\hat{r}_1]) = (a \oplus b)[\widehat{G}]. \quad (195)$$

The elements mapped to zero are exactly those with $a = b$. Hence

$$\ker i_* = \text{span}_{\mathbb{F}_2}\{[\hat{r}_0] \oplus [\hat{r}_1]\} \cong \mathbb{F}_2. \quad (196)$$

By exactness of Eq. (192), the image of ∂_{rel} is equal to $\ker i_*$:

$$\text{im } \partial_{\text{rel}} = \ker i_*. \quad (197)$$

The first zero in Eq. (192) also implies that ∂_{rel} is injective. Therefore

$$H_1(\widehat{G}, A; \mathbb{F}_2) \cong \text{im } \partial_{\text{rel}} = \ker i_*. \quad (198)$$

Using Eq. (196), we obtain

$$H_1(\widehat{G}, A; \mathbb{F}_2) \cong \mathbb{F}_2. \quad (199)$$

For background on relative homology and the homology long exact sequence, see Secs. 8–9 of Haynes Miller's *Lectures on Algebraic Topology*, available at <https://math.mit.edu/~hrm/papers/lectures-905-906.pdf>.

This relative homology group has two classes. The zero class is the class of relative boundaries. Since A has no 1-cells, the relative 1-boundaries are the usual plaquette boundaries:

$$B_1(\widehat{G}, A; \mathbb{F}_2) = \text{im } \widehat{B}. \quad (200)$$

Thus the zero class corresponds to products of Z -type plaquette stabilizers.

The other class is the bridge class. To see this, let \hat{c} be a bridge. Then

$$\widehat{D}\hat{c} = \hat{r}_0 \oplus \hat{r}_1. \quad (201)$$

Therefore the relative boundary map sends its class to

$$\partial_{\text{rel}}[\hat{c}] = [\hat{r}_0] \oplus [\hat{r}_1], \quad (202)$$

which is the nonzero element of $\ker i_*$. Hence $[\hat{c}]$ is nonzero in $H_1(\widehat{G}, A; \mathbb{F}_2)$. Since the group has only one nonzero element, every bridge represents the same nonzero relative class.

In surface-code language, this says that every bridge from R_0 to R_1 is the same nontrivial logical Z -string up to plaquette stabilizers. Indeed, a plaquette boundary has no ordinary boundary, because

$$\widehat{D}\widehat{B} = 0. \quad (203)$$

A bridge has ordinary boundary $\hat{r}_0 \oplus \hat{r}_1$. Therefore a bridge cannot be a product of plaquette stabilizers. It represents the nontrivial logical operator \bar{Z} .

Proposition S4.1 (Fixed holes imply one bridge class). Fix two clean actual rough holes R_0 and R_1 . Let $A = \{\hat{r}_0, \hat{r}_1\}$ be the two marked vertices in the quotient complex \widehat{G} .

Let c and c' be legal Z chains. Then \hat{c} and \hat{c}' are relative 1-cycles for the pair (\widehat{G}, A) . We write

$$[\hat{c}] \in H_1(\widehat{G}, A; \mathbb{F}_2) \quad (204)$$

for the relative homology class of \hat{c} . Equivalently, $[\hat{c}]$ is the coset of \hat{c} modulo relative 1-boundaries.

Then

$$[\hat{c}] = [\hat{c}'] \quad \text{in} \quad H_1(\widehat{G}, A; \mathbb{F}_2) \quad (205)$$

if and only if

$$\hat{c} \oplus \hat{c}' \in \text{im } \widehat{B}. \quad (206)$$

Equivalently, $Z(c)$ and $Z(c')$ differ by Z -type plaquette stabilizers and have the same action on the code space.

In particular, any two bridges from R_0 to R_1 represent the same nonzero relative class. Hence all bridge operators act as the same nontrivial logical operator \bar{Z} .

Proof. We only need to unpack the quotient in the definition of relative homology. By definition,

$$H_1(\widehat{G}, A; \mathbb{F}_2) = Z_1(\widehat{G}, A; \mathbb{F}_2) / B_1(\widehat{G}, A; \mathbb{F}_2). \quad (207)$$

Here $Z_1(\widehat{G}, A; \mathbb{F}_2)$ is the group of relative 1-cycles, namely legal 1-chains whose endpoints lie in A . The subgroup $B_1(\widehat{G}, A; \mathbb{F}_2)$ is the group of relative 1-boundaries.

Thus two legal chains define the same relative class exactly when their difference is a relative boundary:

$$[\hat{c}] = [\hat{c}'] \quad \iff \quad \hat{c} \oplus \hat{c}' \in B_1(\widehat{G}, A; \mathbb{F}_2). \quad (208)$$

All chain groups are over \mathbb{F}_2 , so subtraction is the same as addition.

Since $A = \{\hat{r}_0, \hat{r}_1\}$ has no 1-cells,

$$C_1(A; \mathbb{F}_2) = 0. \quad (209)$$

Therefore the relative 1-boundaries are just the ordinary boundaries of 2-chains in \widehat{G} . These are exactly the plaquette boundaries:

$$B_1(\widehat{G}, A; \mathbb{F}_2) = \text{im } \widehat{B}. \quad (210)$$

Hence

$$[\hat{c}] = [\hat{c}'] \quad \iff \quad \hat{c} \oplus \hat{c}' \in \text{im } \widehat{B}. \quad (211)$$

This gives the stabilizer statement. If

$$\hat{c} \oplus \hat{c}' = \widehat{B}s, \quad (212)$$

then $Z(c)$ and $Z(c')$ differ by the product of the Z -type plaquette stabilizers selected by s . Hence they act in the same way on the code space.

Now let c be a bridge from R_0 to R_1 . Then

$$\widehat{D}\hat{c} = \hat{r}_0 \oplus \hat{r}_1. \quad (213)$$

So $[\hat{c}]$ cannot be the zero class. Indeed, if $[\hat{c}] = 0$, then $\hat{c} \in \text{im } \widehat{B}$, and therefore

$$\widehat{D}\hat{c} = 0, \quad (214)$$

because $\widehat{D}\widehat{B} = 0$. This contradicts

$$\widehat{D}\hat{c} = \hat{r}_0 \oplus \hat{r}_1 \neq 0. \quad (215)$$

By Eq. (199),

$$H_1(\widehat{G}, A; \mathbb{F}_2) \cong \mathbb{F}_2. \quad (216)$$

Thus there is only one nonzero relative class. Since every bridge is nonzero, all bridges represent this same class.

Therefore any two bridge operators differ only by Z -type plaquette stabilizers. They act as the same nontrivial logical operator on the code space. We denote this common logical operator by \bar{Z} . This proves the proposition. \square

Proposition S4.2 (Simple dual witness for fixed holes). Fix the same two clean actual rough holes R_0 and R_1 . Then there exists a simple closed dual loop w that separates R_0 from R_1 . For any such w , every bridge c from R_0 to R_1 satisfies

$$\langle w, c \rangle = 1. \quad (217)$$

Moreover, if \hat{w} is any closed dual 1-cochain with odd pairing with one bridge c_\star , then \hat{w} has odd pairing with every bridge.

Proof. Since R_0 and R_1 are disjoint clean actual rough holes in a planar patch, we may choose a small regular neighborhood $N(R_0)$ of R_0 that does not meet R_1 . We choose it so that its boundary lies on the dual lattice. Because R_0 is disk-like, $N(R_0)$ is also disk-like. Hence its boundary is a simple closed dual loop. Denote this loop by w .

The loop w separates the sphere into two connected components. One component contains R_0 , and the other contains R_1 . Let c be any bridge from R_0 to R_1 . The path c starts on one side of w and ends on the other side. Each crossing with w changes the side of the path. Therefore the number of crossings is odd. Hence

$$\langle w, c \rangle = 1. \quad (218)$$

Now let \hat{w} be any closed dual 1-cochain. The closed condition is

$$\widehat{B}^\top \hat{w} = 0. \quad (219)$$

If two legal chains differ by a plaquette boundary,

$$\hat{c}' = \hat{c} \oplus \widehat{B}s, \quad (220)$$

then

$$\langle \hat{w}, \hat{c}' \rangle = \langle \hat{w}, \hat{c} \rangle \oplus \langle \widehat{B}^\top \hat{w}, s \rangle = \langle \hat{w}, \hat{c} \rangle. \quad (221)$$

Thus the pairing with \hat{w} depends only on the relative homology class of the bridge.

By Proposition S4.1, all bridges from R_0 to R_1 represent the same nonzero relative class. Therefore, if \hat{w} pairs oddly with one bridge c_\star , then it pairs oddly with every bridge. \square

We can now prove the clean puncture realization statement used in the main text.

Proof of the clean puncture realization proposition.

Assume first that a global odd witness has been locally realized by two clean actual rough holes R_0 and R_1 . Let \widehat{G} be the quotient complex obtained by collapsing R_0 and R_1 to two marked vertices \hat{r}_0 and \hat{r}_1 . Set

$$A = \{\hat{r}_0, \hat{r}_1\}. \quad (222)$$

By the clean condition, each prescribed signal chain c_α has one endpoint on the rough boundary of R_0 and one endpoint on the rough boundary of R_1 . Its interior stays in the active code region. Therefore, after the quotient, \hat{c}_α has ordinary boundary

$$\widehat{D}\hat{c}_\alpha = \hat{r}_0 \oplus \hat{r}_1 \quad \text{for all } \alpha. \quad (223)$$

Since this boundary lies in $C_0(A; \mathbb{F}_2)$, each \hat{c}_α is a relative 1-cycle for the pair (\widehat{G}, A) .

Choose one reference signal chain and call it c_\star . By Proposition S4.1, all bridges from R_0 to R_1 represent the same nonzero class in

$$H_1(\widehat{G}, A; \mathbb{F}_2). \quad (224)$$

Hence

$$[\hat{c}_\alpha] = [\hat{c}_\star] \neq 0 \quad \text{for all } \alpha. \quad (225)$$

By the definition of relative homology, two relative 1-cycles represent the same class if and only if their difference is a relative 1-boundary. Here all groups are over \mathbb{F}_2 , so difference is the same as XOR. Since A has no 1-cells, the relative 1-boundaries are exactly the ordinary plaquette boundaries in \widehat{G} . Therefore

$$\hat{c}_\alpha \oplus \hat{c}_\star \in \text{im } \widehat{B} \quad \text{for all } \alpha. \quad (226)$$

Equivalently, for each α , there exists a 2-chain s_α such that

$$\hat{c}_\alpha \oplus \hat{c}_\star = \widehat{B}s_\alpha. \quad (227)$$

This is exactly the stabilizer equivalence. The operator $Z(c_\alpha)Z(c_\star)$ is the product of the Z -type plaquette stabilizers selected by s_α . Therefore $Z(c_\alpha)$ and $Z(c_\star)$ have the same action on the code space:

$$P_C Z(c_\alpha) P_C = P_C Z(c_\star) P_C \quad \text{for all } \alpha. \quad (228)$$

Moreover, $[\hat{c}_\star] \neq 0$. Thus c_\star is not a plaquette boundary. Hence $Z(c_\star)$ is not a Z -type stabilizer. Since c_\star is a legal bridge, it commutes with all active star checks and preserves the code space. Therefore it is a nontrivial logical Z operator. We denote its logical action by \bar{Z} . Thus

$$P_C Z(c_\alpha) P_C = P_C Z(c_\star) P_C \neq 0 \quad \text{for all } \alpha. \quad (229)$$

This proves the forward direction.

Conversely, suppose that two clean actual rough holes R_0 and R_1 are fixed. Suppose also that there is a reference path c_\star from R_0 to R_1 such that every c_α represents the same nonzero bridge class:

$$[\hat{c}_\alpha] = [\hat{c}_\star] \neq 0 \quad \text{for all } \alpha. \quad (230)$$

Then each c_α is a bridge from R_0 to R_1 .

By Proposition S4.2, we may choose a simple closed dual loop w separating R_0 from R_1 . Every bridge from R_0 to R_1 crosses this loop with odd parity. Hence

$$\langle w, c_\alpha \rangle = 1 \quad \text{for all } \alpha. \quad (231)$$

Thus the fixed nonzero bridge class admits a simple odd dual witness. Since R_0 and R_1 are clean by assumption, the data

$$(w, \Omega_0, \Omega_1, R_0, R_1) \quad (232)$$

form a clean witness configuration for these fixed holes.

This proves the proposition. \square

The quotient notation should not be read as a physical operation. It is only a way to treat all allowed endpoints on the same rough boundary as one marked point. Physically, a Z string terminates on the rough boundary of the actual rough hole. Its interior remains in the active code region.

The relative homology group $H_1(\widehat{G}, A; \mathbb{F}_2)$ has only one nonzero element. This is why the proof is strong. It does not depend on the shape, length, or microscopic route of a bridge. Once a legal Z string connects R_0 to R_1 , it is in the unique nonzero class and acts as the same logical \bar{Z} .

SUP5 SURFACE-CODE REALIZATION OF THE LOGICAL RAMSEY PROTOCOL

In this section we connect the topological construction in SUP2–SUP4 to the optimal GHZ-type protocol for quantum sensor networks developed in Ref. [2]. The goal is to estimate one weighted linear functional of many unknown couplings,

$$q = \sum_{\alpha \in I} s_\alpha \lambda_\alpha. \quad (233)$$

The surface-code protocol has the same logical structure as the GHZ protocol. The difference is where the phase is stored. In the usual network protocol, the phase is stored in a GHZ subspace. Here, it is stored in one protected logical qubit of a punctured surface code.

Assume that the clean puncture construction has succeeded. Thus we have two clean actual rough holes R_0 and R_1 . The corresponding punctured code has code space C and projector P_C .

Let $\{c_\alpha : \alpha \in \mathcal{I}\}$ be the prescribed signal chains. By the clean puncture realization proved in SUP4, every c_α is a legal bridge from R_0 to R_1 . Moreover, all these bridges represent the same nonzero relative homology class. Hence there is a reference path c_\star such that

$$P_C Z(c_\alpha) P_C = P_C Z(c_\star) P_C \neq 0 \quad \text{for all } \alpha \in \mathcal{I}. \quad (234)$$

We choose

$$\bar{Z} := Z(c_\star) \quad (235)$$

as a representative of the logical Z operator. Then Eq. (234) becomes

$$P_C Z(c_\alpha) P_C = P_C \bar{Z} P_C \quad \text{for all } \alpha \in \mathcal{I}. \quad (236)$$

This is the only topological input needed in this section.

We use the same normalization as in the main text:

$$|s_\alpha| \leq 1 \quad \text{for all } \alpha, \quad \max_\alpha |s_\alpha| = 1. \quad (237)$$

This normalization only fixes the scale of the target functional. If the original weights are \tilde{s}_α , then one first divides all weights by $\max_\alpha |\tilde{s}_\alpha|$ and rescales the final estimate back at the end.

We now include control through signed activation profiles. During the sensing window $0 \leq t' \leq T$, let

$$\eta_\alpha(t') \in [-1, 1] \quad (238)$$

be the signed activation strength of the signal chain c_α . In a bang-bang implementation one may take

$$\eta_\alpha(t') \in \{-1, +1\}. \quad (239)$$

The value $+1$ means that the signal is active with its original sign. The value -1 means that an echo operation reverses the sign.

The controlled sensing Hamiltonian is

$$H_{\text{sig}}(t') = \frac{1}{2} \sum_{\alpha \in \mathcal{I}} \eta_\alpha(t') \lambda_\alpha Z(c_\alpha). \quad (240)$$

Using Eq. (236), its restriction to the code space is

$$P_C H_{\text{sig}}(t') P_C = \frac{1}{2} \left(\sum_{\alpha \in \mathcal{I}} \eta_\alpha(t') \lambda_\alpha \right) P_C \bar{Z} P_C. \quad (241)$$

All signal terms are Z -type terms, so they commute with one another. Thus there is no time-ordering issue. The logical evolution generated during the sensing part of the schedule is

$$U_{\text{log}}(T) = \exp \left[-\frac{i}{2} \left(\sum_{\alpha \in \mathcal{I}} \lambda_\alpha \int_0^T \eta_\alpha(t') dt' \right) \bar{Z} \right]. \quad (242)$$

The schedule realizes effective logical time t for the target q if

$$\int_0^T \eta_\alpha(t') dt' = t s_\alpha \quad \text{for all } \alpha \in \mathcal{I}. \quad (243)$$

When this condition holds,

$$U_{\text{log}}(T) = \exp \left[-\frac{it}{2} \left(\sum_{\alpha \in \mathcal{I}} s_\alpha \lambda_\alpha \right) \bar{Z} \right] = \exp \left(-\frac{it}{2} q \bar{Z} \right). \quad (244)$$

We first consider parallel loading. In this case the two rough holes are fixed, and several compatible signal chains contribute during the same sensing window. Since $|\eta_\alpha(t')| \leq 1$, Eq. (243) implies

$$T_{\text{par}} \geq t|s_\alpha| \quad \text{for every } \alpha. \quad (245)$$

Therefore

$$T_{\text{par}} \geq t \max_\alpha |s_\alpha|. \quad (246)$$

Using the normalization in Eq. (237), this gives

$$T_{\text{par}}^{\min} = t. \quad (247)$$

This lower bound is achieved by time-averaged echo control. For example, if $T_{\text{par}} = t$, a coefficient s_α can be realized by choosing $\eta_\alpha(t') = +1$ for a fraction $(1 + s_\alpha)/2$ of the sensing time and $\eta_\alpha(t') = -1$ for the remaining fraction $(1 - s_\alpha)/2$. Then

$$\int_0^{T_{\text{par}}} \eta_\alpha(t') dt' = ts_\alpha. \quad (248)$$

We next recall the sequential version. This is the setting justified in SUP1. The rough holes are moved through a sequence of code configurations. At dwell step r , one intended signal chain c_r is legal for the current code configuration. After the known Pauli-frame identification between consecutive code spaces, this chain represents the same logical operator \bar{Z} .

Suppose step r senses the coupling λ_{α_r} for dwell time τ_r . Let

$$\sigma_r \in \{\pm 1\} \quad (249)$$

record whether an echo reverses the sign. Then the logical contribution of this dwell step is

$$H_{\text{eff}}^{(r)} = \frac{1}{2} \sigma_r \lambda_{\alpha_r} \bar{Z}. \quad (250)$$

The total sequential dwell time is

$$T_{\text{seq}} = \sum_r \tau_r. \quad (251)$$

To realize Eq. (244), the dwell times must satisfy

$$\sum_{r:\alpha_r=\alpha} \sigma_r \tau_r = ts_\alpha \quad \text{for every } \alpha. \quad (252)$$

For a fixed α , the total unsigned dwell time assigned to λ_α is at least $t|s_\alpha|$. Hence

$$T_{\text{seq}} \geq t \sum_{\alpha \in \mathcal{I}} |s_\alpha|. \quad (253)$$

The bound is reached when each coefficient is implemented with the minimal signed dwell time. Therefore

$$T_{\text{seq}}^{\min} = t \sum_{\alpha \in \mathcal{I}} |s_\alpha|. \quad (254)$$

Thus sequential hole motion generally takes longer dwell time than parallel loading. For an equal-weight sum over M couplings, the slowdown factor is M .

We now give the Ramsey readout. Prepare the logical $+1$ eigenstate of \bar{X} ,

$$|+_L\rangle = \frac{1}{\sqrt{2}} (|0_L\rangle + |1_L\rangle). \quad (255)$$

After the logical evolution in Eq. (244), the state is

$$|\psi(q; t)\rangle = \exp\left(-\frac{it}{2} q \bar{Z}\right) |+_L\rangle = \frac{1}{\sqrt{2}} \left(e^{-iqt/2} |0_L\rangle + e^{+iqt/2} |1_L\rangle \right). \quad (256)$$

This has the same form as the GHZ phase state in the usual sensor-network protocol. In the GHZ protocol, the two-dimensional subspace is spanned by $|0\rangle^{\otimes M}$ and $|1\rangle^{\otimes M}$. Here, the two-dimensional subspace is the logical code space spanned by $|0_L\rangle$ and $|1_L\rangle$.

Finally measure \bar{X} . The two outcomes have probabilities

$$p_+(q) = \cos^2\left(\frac{qt}{2}\right), \quad p_-(q) = \sin^2\left(\frac{qt}{2}\right). \quad (257)$$

The classical Fisher information for estimating q from this binary distribution is

$$F(q) = \sum_{\mu \in \{+, -\}} \frac{(\partial_q p_\mu(q))^2}{p_\mu(q)} = t^2. \quad (258)$$

For ν independent repetitions, the Cramér–Rao bound gives

$$\text{Var}(Q) \geq \frac{1}{\nu t^2}. \quad (259)$$

Thus the achievable error scaling for the target functional is

$$\Delta q \sim \frac{1}{\sqrt{\nu} t}. \quad (260)$$

This is the same scaling as the optimal GHZ protocol for estimating one linear functional.

As a useful special case, suppose the target is the average of M local couplings. We first estimate

$$q_{\text{sum}} = \sum_{\alpha=1}^M \lambda_\alpha, \quad (261)$$

and then divide by M :

$$\bar{\lambda} = \frac{q_{\text{sum}}}{M}. \quad (262)$$

From Eq. (259),

$$\text{Var}(\bar{\Lambda}) = \frac{\text{Var}(Q_{\text{sum}})}{M^2} \geq \frac{1}{\nu M^2 t^2}. \quad (263)$$

Here, $\bar{\Lambda} := Q_{\text{sum}}/M$ is the corresponding estimator of $\bar{\lambda}$. Equivalently,

$$\Delta \bar{\lambda} \sim \frac{1}{\sqrt{\nu} M t}. \quad (264)$$

The factor M appears because the parameter of interest is a nonlocal average. If the goal were to estimate one local coupling alone, this global encoding would not give an M -fold improvement.

We close with the security intuition. Let A be a correctable region of the punctured code. Then every operator supported on A acts trivially on the logical qubit. Equivalently, for any operator O_A supported on A ,

$$P_C O_A P_C = c(O_A) P_C \quad (265)$$

for some scalar $c(O_A)$. Therefore, measurement statistics available inside A are independent of the logical state. In particular, they are independent of the phase q in Eq. (256). To learn q , one must measure a logical observable such as \bar{X} , which is nonlocal at the physical level. This is the surface-code analogue of the security intuition of the GHZ protocol.

In summary, SUP2 gives the global odd-witness criterion, SUP3 explains how simple witnesses guide the clean hole construction, and SUP4 proves that fixed clean rough holes turn all legal bridges into the same nonzero logical \bar{Z} . SUP5 then shows that the compatible many-body Z signals reduce to one logical Ramsey phase, leading to a Fisher information t^2 for the target functional.

SUP6 NO-GO FOR TWO-QUBIT OVERLAPS OF THREE-BODY Z SIGNALS

In the main text we also discuss three-body Z signals with overlapping supports. Here we prove the basic algebraic rule used there. The rule is simple: two distinct three-body Z signals cannot share two data qubits if they are required to act as the same logical \bar{Z} on the code space.

The proof uses only stabilizer algebra. It does not use the witness construction from SUP2–SUP4, nor the Ramsey protocol from SUP5.

We keep the notation from SUP1–SUP5. Data qubits live on edges E . A Z -type Pauli operator is specified by a binary 1-chain

$$c \in C_1(G; \mathbb{F}_2) \cong \mathbb{F}_2^E. \quad (266)$$

We write

$$Z(c) := \prod_{e:c_e=1} Z_e. \quad (267)$$

The support size is

$$|c| := \sum_{e \in E} c_e. \quad (268)$$

A three-body signal has $|c| = 3$. We denote the stabilizer group by \mathcal{S} , the code space by \mathcal{C} , and the code projector by $P_{\mathcal{C}}$.

We will use one elementary property of the surface-code patches considered in this work. A Z -type stabilizer is a product of Z -plaquette checks. Equivalently, in chain notation its support is a plaquette-boundary sum. For the ordinary planar patches used here, no nonzero Z -type stabilizer has weight two.

Proposition S6.1 (Two-qubit overlap no-go). Let $c_a, c_b \in C_1(G; \mathbb{F}_2)$ satisfy

$$|c_a| = |c_b| = 3. \quad (269)$$

Assume that the two signal operators act identically and nontrivially on the code space:

$$P_{\mathcal{C}}Z(c_a)P_{\mathcal{C}} = P_{\mathcal{C}}Z(c_b)P_{\mathcal{C}} \neq 0. \quad (270)$$

Then either $c_a = c_b$, or the two supports overlap on at most one data qubit. Equivalently, if $c_a \neq c_b$, then

$$|\text{supp}(c_a) \cap \text{supp}(c_b)| \leq 1. \quad (271)$$

Proof. First note that Eq. (270) implies that both $Z(c_a)$ and $Z(c_b)$ preserve the code space. Indeed, if a Pauli operator anticommutes with some stabilizer generator, then it maps \mathcal{C} to an orthogonal syndrome sector, and its code-space projection is zero. Since the two projections in Eq. (270) are nonzero, both operators lie in the normalizer $\mathcal{N}(\mathcal{S})$.

Define

$$Q := Z(c_a)Z(c_b). \quad (272)$$

Since $Z(c_a)$ and $Z(c_b)$ commute with $P_{\mathcal{C}}$, we have

$$\begin{aligned} P_{\mathcal{C}}QP_{\mathcal{C}} &= P_{\mathcal{C}}Z(c_a)Z(c_b)P_{\mathcal{C}} \\ &= P_{\mathcal{C}}Z(c_a)P_{\mathcal{C}}Z(c_b)P_{\mathcal{C}} \\ &= P_{\mathcal{C}}Z(c_b)P_{\mathcal{C}}Z(c_b)P_{\mathcal{C}} \\ &= P_{\mathcal{C}}Z(c_b)^2P_{\mathcal{C}} \\ &= P_{\mathcal{C}}. \end{aligned} \quad (273)$$

Thus Q acts as the identity logical operator on \mathcal{C} . In a stabilizer code, this means that Q is a stabilizer, up to an overall Pauli phase.

Since Q is Z -type, it must be a Z -type stabilizer. Therefore its support must be a product of plaquette boundaries.

Because both factors are Z -type, their product cancels on the overlap:

$$Q = Z(c_a)Z(c_b) = Z(c_a \oplus c_b), \quad (274)$$

where \oplus denotes addition over \mathbb{F}_2 . Let

$$r := |\text{supp}(c_a) \cap \text{supp}(c_b)|. \quad (275)$$

Since $|c_a| = |c_b| = 3$, we get

$$|c_a \oplus c_b| = |c_a| + |c_b| - 2r = 6 - 2r. \quad (276)$$

If $r = 3$, then $|c_a \oplus c_b| = 0$, so $c_a = c_b$.

If $r = 2$ and $c_a \neq c_b$, then

$$|c_a \oplus c_b| = 2. \quad (277)$$

In this case $Q = Z(c_a \oplus c_b)$ is a nontrivial weight-two Z operator. But a nonzero weight-two Z operator cannot be a Z -type stabilizer on the surface-code patches considered here. A Z -type stabilizer is a plaquette boundary sum, and such a support cannot have weight two.

This contradicts Eq. (273). Hence the case $r = 2$ is impossible for two distinct three-body signals.

Therefore, if $c_a \neq c_b$, the overlap size must satisfy

$$r \leq 1. \quad (278)$$

This proves the proposition. \square

Proposition S6.1 gives the first practical rule for the overlapping-support regime. If several three-body Z signals are required to compress to one logical Z , then two distinct signal terms may share at most one data qubit. A two-qubit overlap would make the product of the two signals a nontrivial weight-two Z operator. Such an operator cannot be the stabilizer needed to make the two signals logically identical.

More generally, the same stabilizer argument is not special to three-body signals. For arbitrary Z -type signal supports, logical equivalence forces

$$Z(c_a \oplus c_b) \quad (279)$$

to be a Z -type stabilizer, up to phase. Thus two distinct local terms cannot overlap so much that their symmetric difference becomes too small to form a valid plaquette-boundary support.